Investigation of orographically induced rainfall over Western Ghats and its association with other monsoon parameters

Thesis submitted to the Andhra University, Visakhapatnam
in partial fulfilment of the requirement for the award of
Master of Technology in Remote Sensing and GIS

Submitted By:

Sayli Atul Tawde

Supervised By:

Ms. Charu Singh

Indian Institute of Remote Sensing, ISRO,
Dept. of Space, Govt. of India, Dehradun – 248001
Uttarakhand, India

August, 2013

Acknowledgement

This thesis arose in part of my M. Tech. project work that has been carried out at Indian Institute of Remote Sensing. The guidance and support of people in the making of the thesis deserve a special mention. It is a pleasure to convey my gratitude to them all in my humble acknowledgement.

At this moment of accomplishment, first of all I am extremely indebted to my guide, Ms. Charu Singh, Scientist 'SD', MASD, IIRS. This work would not have been possible without her valuable guidance and support. Under her guidance I successfully overcame many difficulties and learned a lot. She has given me a freedom to make mistakes and learn new things throughout the project. I gratefully acknowledge her valuable suggestions not only bounded for my project work but also for my better career prospective in the field of atmospheric sciences. Her conviction will always inspire me to work hard.

I am thankful to Dr. D. Mitra, Head MASD, Ms. Shefali Agarwal, M. Tech. Course coordinator and Head PRSD, Dr. S. K. Saha ,Group Director ER & SS Group and Dean (Academics) IIRS, and Dr. Y. V. N. Krishna Murthy , Director IIRS for their valuable advices, and support during my project work.

The fruitful discussion during project work with Dr. Bhaskar R. Nikam and Dr. Shuchita Srivastava is highly acknowledged.

A sincere gratitude to Negi mam, Kamlesh mam, Shrinivasa Raju sir, Kailash sir for providing required help to access library facilities and to all members of CMA for maintaining computer systems including software installation in MASD lab during the project work.

I pay homage to the Indian Institute of Remote Sensing, Dehradun for providing necessary infrastructure and resources to learn and accomplish the M.Tech. course in Remote Sensing & GIS. My sincere thanks to Andhra University, Visakhapatnam for awarding me this opportunity.

I extend my thanks to all following organization that have been providing satellite and in-situ data sets for research purpose. I would like to thank National Data Centre, IMD, Pune for supplying rain gauge data used for the analysis. TRMM 3B42 v7 data used in this study were acquired from GES-DISC Interactive Online Visualization and Analysis Infrastructure (Giovanni; as part of the NASA's Goddard Earth sciences (GES) Data and Information Services Centre (DISC)). ASTER GDEM is a product of METI and NASA . I am grateful to METI and NASA for providing online DEM data for research purpose. WINDSAT data are

produced by Remote Sensing Systems and sponsored by the NASA Earth Science Measures Discover Project and the NASA Earth Science Physical Oceanography Program. My sincere expression of thanks to ISRO data portal MOSDAC for providing Indian satellite and in-situ data for research purpose.

I owe gratitude to Dr. Pramod Kale and Dr. Hemchandra Pradhan for encouraging me to pursue M. Tech. degree in Remote Sensing and GIS.

My deep sense of gratitude towards my friend Sharath Chowdappa, for helping and encouraging me willingly and selflessly during my research endeavor.

My warm appreciations to Ms. Shailja and my colleague Lekshmi for giving fruitful suggestions whenever needed during my project work.

I owe a special gratitude to my loving sister Chandana, my parents and grandparents for advising, educating and awarding me independence till now. I owe everything to them.

Besides this, I thank several people have knowingly and unknowingly helped me in the successful completion of this project.

CERTIFICATE

This is to certify that ***Ms. Sayli Atul Tawde*** has carried out the dissertation entitled ***"Investigation of orographically induced rainfall over Western Ghats and its association with other monsoon parameters"*** in partial fulfilment of the requirements for the award of ***M. Tech in Remote Sensing and GIS***. This work has been carried out under the supervision of ***Ms. Charu Singh,*** Scientist 'SD', Marine and Atmospheric Sciences Department, Indian Institute of Remote Sensing, ISRO, Dehradun, Uttarakhand, India.

Ms. Charu Singh
Project Supervisor
Marine & Atmospheric Sciences Department
IIRS, Dehradun

Dr. Debashis Mitra
Head
Marine & Atmospheric Sciences Department
IIRS, Dehradun

Dr. S. K. Saha
Group Director ER & SS Group & Dean (Academics)
IIRS, Dehradun

Dr. Y.V.N. Krishna Murthy
Director,
IIRS, Dehradun

Declaration

I, ***Sayli Atul Tawde***, hereby declare that this dissertation entitled "***Investigation of orographically induced rainfall over Western Ghats and its association with other monsoon parameters****"* submitted to Andhra University, Visakhapatnam in partial fulfilment of the requirements for the award of ***M. Tech in Remote Sensing and GIS Application***, is my own work and that to the best of my knowledge and belief. It is a record of original research carried out by me under the guidance and supervision of **Ms. Charu Singh**, Scientist 'SD', MASD, Indian Institute of Remote Sensing, Dehradun. It contains no material previously published or written by another person nor material which to a substantial extent has been accepted for the award of any other degree or diploma of the university or other institute of higher learning, except where due acknowledgment has been made in the text.

Place: Dehradun Ms. Sayli Atul Tawde

Date:

Dedicated to

my Aai and Baba,
sister Chandana

for their encouragement and inspiration
throughout my project work and
lifting me uphill in this phase of life.

Abstract

The study ratiocinate local forcing of static as well as some dynamic parameters on enhanced rainfall over Western Ghats (WG) of India during south west Monsoon. Using remotely sensed TRMM 3B42 v7 rainfall and topographic data from ASTER DEM (Digital Elevation Model), the impact of orographical aspects like topography, spatial variability in elevation and slope are examined to investigate capacious Indian Summer Monsoon Rainfall (ISMR) over WG. In addition to this attempts have been made to analyse the variations in precipitation with respect to the sea surface temperature (SST) of Arabian Sea (AS), wind speed (WS); ENSO (El Nino Southern Oscillations) cycle and Indian Ocean Dipole (IOD) event. Comparing topography of various states in WG, it has been observed that Karnataka receives highest mean monsoon rainfall over WG during summer monsoon. The results ascertain that the orographic precipitation is a coupled output of topography (width and length), slope and elevation of the mountain barrier. Longer and broader i.e. cascaded topography, heighted summits and gradually increasing slopes impel the enhancement in precipitation. A sharp abatement in rainfall before the peak of mountains has been discovered. In addition to this, the spatial distribution of heavy rainfall events during the last 14 years has also been explored. The association of the SST & low level winds over AS with the enhanced monthly and seasonal precipitation over WG could not be ascertained; however, the daily rainfall found to be significantly modulated by AS SST and WS fluctuations. AS state and WS conditions prior to the heavy downpour have been pragmatically identified. The interannual variability of rainfall during monsoon season over WG is observed to be associated with ENSO cycle and Indian Ocean dipole. The correlation between ENSO-ISMR and IOD-ISMR over WG is negative and positive respectively but insignificant. The analysis of interannual variation of frequency of extreme rain events over WG shows that extreme rain events over WG are independent from the large scale forcing (for example – ENSO and IOD), unlike dependency of no. of extreme rain events over central India. The correlation coefficient between ENSO & no. of extreme events over WG is -0.4642 (significant at 9% significance level) while with IOD it is found to be -0.5394 (significant at 6% significance level) for last 14 years. The results presented in this study are statistically significant. Present work would help policy makers to manage the hazard scenario and also to strengthen the prediction skills over mountainous terrain of WG.

Table of content

List of figures:

List of tables:

Chapter 1. Introduction

1.1 Process and places associated with orographic precipitation

Western Ghats and North-East region of India are the two locations which receive highest annual rainfall in India (fig. 1.1). Both of these regions have unique characteristic of mountainous terrain. This hilly terrain acts as a hermetic to south west winds coming from AS leading to intensified downpour at the windward side of the mountains. This type of rainfall is known as 'orographic rainfall'. The term orography refers to study of physical geography of mountains i.e. it examines natural phenomenon with respect to variation in length, width, height, location of mountain. Over Indian subcontinent the enhanced precipitation due to orography is observed prominently in south west monsoon season. The large sea breezes flow from ocean towards land during monsoon season due to differential heating of land and adjacent ocean in tropical regions. This seasonal heating results in development of thermal low over continent leading to strong westerly winds prevailing Indian region. The encroachment of a large scale flow from the ocean towards the land is primarily due to pressure gradient between land and ocean surfaces. When this moist flow reaches near the land it gets modified due to local topography of the region. Small scale flow interacts first with the mountainous terrain and forced up by the natural barrier. Amount of rainfall is determined by many factors like availability moisture, wind velocity, wind direction and orography of the region. It indicates static parameter like local topography influences the climate of the region. An orographically induced contrast in precipitation has been observed in many parts of the globe and has become an inquisitive research topic. Smith & Lin (1982) stated that spatial pattern of rainfall of the globe is highly governed by the orography. Some of the famous places for orographically induced precipitation are given below. The Rocky Mountains are a major mountain range in western North America extended in north south direction. Moist air prevails from Northern Pacific ocean and hits the Rockies mountain barrier to give heavy downpour (Smith & Evans, 2007). Also the rainfall contrast has been noted at Washington and Oregon due to north south cascaded mountain range in North America (Moran & Morgan, 1997). In South America, Andes is the north south mountain range proximity to the South Pacific Ocean (fig. 1.2). An asymmetric distribution of precipitation over Andes is found to be greatly dependent on altitude, latitude of mountains. Hawaii is the largest island at the south eastern most location in a chain of volcanic islands in the North Pacific Ocean (fig. 1.3). The effectively blocking of prevailing northeast trade wind reaching the eastern side of the island induces heavy precipitation to the eastern edge of island (Yang & Chen, 2008). Also some studies on a small island in Caribbean Sea named Dominica observed high precipitation due to orographic lifting (Smith et al., 2008). Similarly the above mentioned locations, the Western Ghats (WG) of India (a *World's Heritage Site* owes its rich biodiversity, and flora-fauna due to vast geographic area), is also a varied topographic mountainous region which receives enhanced precipitation during Indian summer monsoon season.

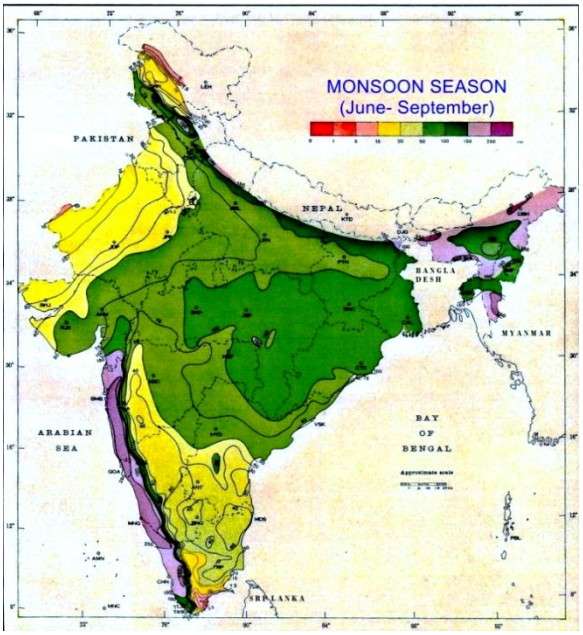

Figure 1.1 Summer monsoon seasonal rainfall distribution of India. Pink colour indicates highest rainfall value. [adopted from http://www.imd.gov.in]

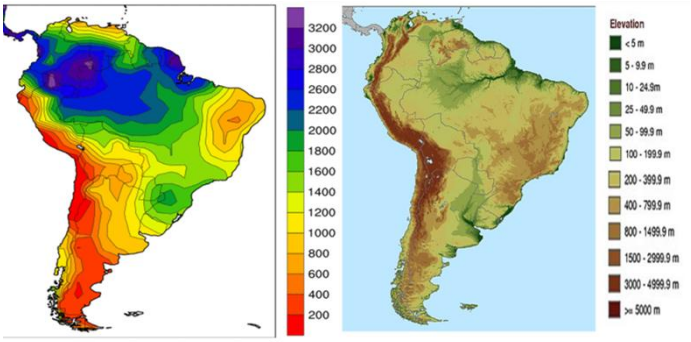

Figure 1.2 North America: Annual rainfall in millimetres (left) and elevation data in meter (right). [http://sedac.ciesin.columbia.edu/data/set/nagdc-population-landscape-climate-estimates-v2/maps]

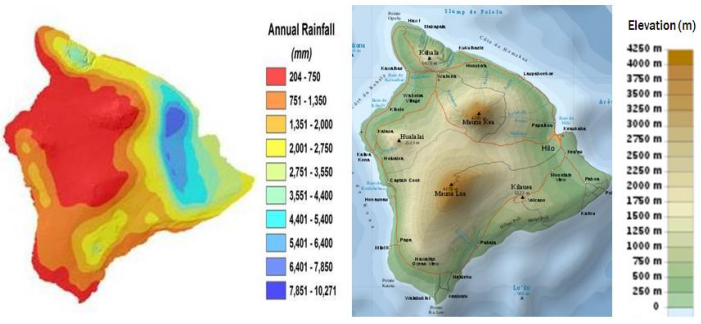

Figure 1.3 Hawaii Island: Annual rainfall in millimetres (left) and elevation data in meter (right). [http://www.google.co.in/search?q=hawaii+island+elevation&tbm=isch&tbo=u&source=univ&sa=X&ei=T1LFUYewIMuGrAe-zIHYCA&ved=0CEcQsAQ&biw=1280&bih=933#imgdii=_]

Accurate prediction over mountainous regions has been an enigma for atmospheric scientists therefore to analyse the impact of the static forcing due to natural mountain barrier on precipitation is necessary for better hazard management in future.

In general, there are three primary lifting processes which cause air to rise and precipitate.

a. Convectional precipitation: vertical circulation of air parcels

b. Frontal precipitation: along the surface of warm/cold front

c. Orographic precipitation: forced ascent of air over mountain slope

The orographic lifting occurs when air is compelled upward by the topography of respective region. There are several mechanisms of orographic lifting (listed below with respective figures i.e. fig. 1.4).

c.1 Stable ascent: Deep upliftment of moist air along windward slope of mountain. This is most common mechanism of orographic precipitation. If the air is moist and convection is sufficiently deep the precipitation cloud forms.

c.2 Seeder-feeder mechanism: Precipitation augments through rapid growth of crystals falling from upper stratiform clouds into the lower orographically induced convective clouds. While downfall ice crystals acts as a condensation nuclei to lower level supercooled water droplets and grow by accretion and aggregation.

c.3 Upslope release of potential instability: Shallow layers of potentially unstable air grow by convection over a mountain.

c.4 Day time convergence: In absence of strong winds, topographic boundary layer flow developed due to day time heating of mountain slopes. This leads to convergence at the top of the mountain.

c.5 Triggering of convergence at lee side: Stable air (Froude number <1), may be forced to travel around the lee ward side of the mountain and this lee ward convergence enhances precipitation on lee ward side of the mountain.

c.6 Enhancement of convergence at lee side: Lee side convergence develops warm convection of air mass at low levels. The mountain driven upper level cold air masses are many times separated from these warm air masses by thin stable layer. This generates extreme unstable condition and heightens convection.

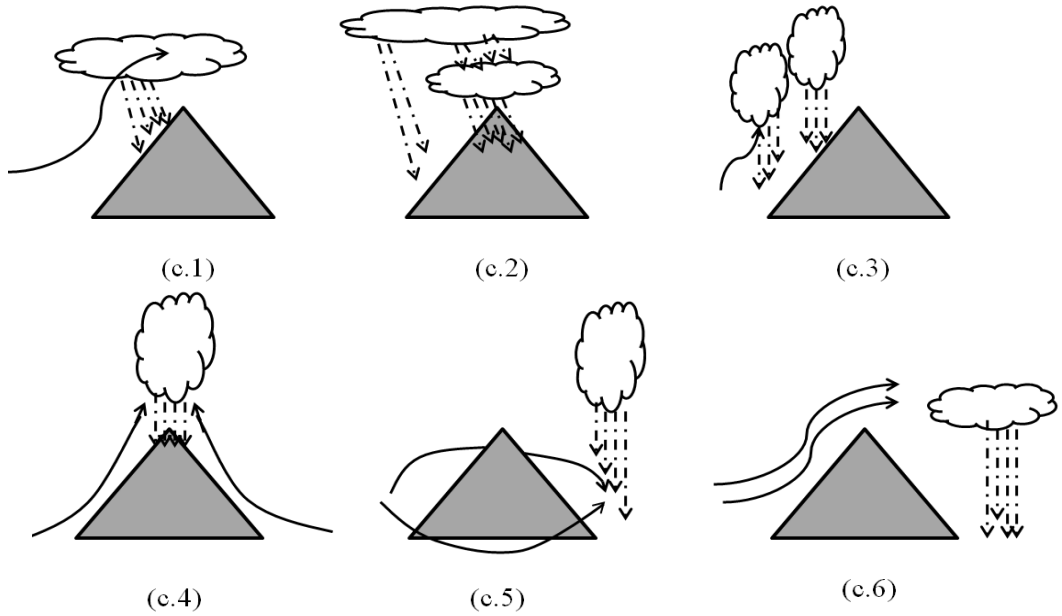

Figure 1.4 Different mechanisms of orographic upliftment.

The stable ascent mechanism of orographic precipitation is explained in the next section.

If the relief of land is sufficiently large the ascending air experiences exponential cooling with increasing height on windward side of the mountain. As moist air parcel rises it feels less surrounding environmental pressure. To equalize with this low pressure, air parcel undergoes adiabatic expansion. In this process air parcel loses its temperature. If environmental is cooler than air parcel, air parcel will travel further in upward direction (unstable atmosphere). As ascending air cools its relative humidity increases. When relative humidity reaches to 100%, air parcel undergoes condensation and precipitation. Therefore the windward side of mountain receives precipitation. The Relative Humidity (R.H.) is discussed by Wallace & Hobbs (2006) as

$$Relative\ humidity = \frac{actual\ \ mixing\ \ ratio}{saturated\ \ \ mixing\ \ ratio} \qquad (1.1)$$

Saturated mixing ratio is the maximum concentration of water vapour in a given volume of air at given temperature. The elevation at which air becomes saturated and cloud forms is known as lifting condensation level (LCL). During the intervening time, the dry air after downpour on windward side descends on the leeward side. While descending on downwind side the air parcel gets compressed and warm. It reduces relative humidity of the parcel and cloud formation ceases. This mechanism introduces the two contrast climate zones i.e. moist and cloudy on windward side and dry, clear on leeward side of the mountain range. This dry condition at lee ward side is known as 'rain shadow' region (Moran & Morgan, 2007).

Orographic precipitation depends on static stability of the atmosphere, wind speed, wind direction and on the topography of the mountain. When incoming air parcel with wind velocity (u) encounters a mountain barrier (height, h) the following mechanisms can occur. Air parcel can pass over a mountain top or it can rest on the mountain top or unable to cross the mountain top (fig. 1.5). The phenomenon that the air parcel remains on the windward side of the mountain

barrier is known as 'blocking of the flow'. Blocking due to orography occurs when Froude number is less than one i.e. stratified atmosphere or weak wind speed. When Froude number is greater than one air flow crosses the mountain top. Froude number (F) is given by following formula:

$$F = \frac{u}{N.h} \quad (1.2)$$

Where N= Brunt Vaisalla frequency [http://meted.ucar.edu]

Brunt Vaisalla frequency determines the stability of the atmosphere. Stability is the restoring force acting on the uplifted air parcel and it depends on the temperature difference of dry air and ambient air. Higher N indicates high static stability of the atmosphere i.e. air parcel oscillates around its equilibrium position. Heavy downpour due to orography is associated with atmospheric blocking (F<1). This blocking is generally initialized by stratification or temperature inversion layer or weak wind speed.

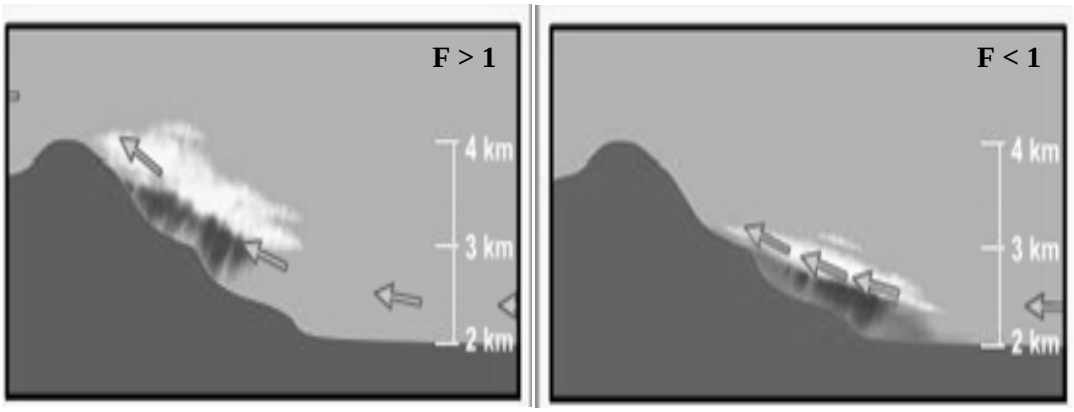

Figure 1.5 Air flow interaction with topography of mountain using Froude number. [http://meted.ucar.edu]

While moving up over mountain slope air parcel has to do work against the gravitational pull. This reduces its energy to travel further up. In the process of condensation to precipitation formation, vertical movement inside the cloud should be sufficient enough to grow water droplets by collision-coalescence. This diminution/ increment in the vertical movement are also decided by the physical features of the mountain barrier. Therefore, the influence of orographical parameters on rainfall intensity has been emphasised in the present study.

1.2 Association of Indian Summer Monsoon with Pacific and Indian Ocean variability

Rainfall regime of any region is an output of local as well as global ocean- atmospheric circulations. The local forcing over WG is due to the orography of that region as well as influence of adjacent AS parameters (for example SST, WS). As summer monsoon season progresses, SST warms in Indian Ocean and this warm pool (SST>28°C) occupies large region in AS and Bay of Bengal. AS is one of the warmest region of world oceans in April-May period (Jaswal et al., 2012). During monsoon, SST cooler anomaly observed over AS. The strength of ISMR is prominently determined by SST (Sengupta et al, 2001; Izumo et al.,2008;

Krishnmurthy & Kirtman, 2002). The global circulation includes El Nino/ La Nina ocean atmospheric interaction (ENSO) in Pacific Ocean and Indian Ocean dipole (IOD) in Indian Ocean. During El Nino, equatorial precipitation tends to be enhanced while during La Nina, less precipitation is observed at the equator and enhanced precipitation near Pacific Northwest region. ENSO has a significant impact on the Indian monsoon region. In general, El Niño events are associated with drought while La Nina events are associated with flood over Indian subcontinent. These fluctuations in equatorial Pacific Oceans cause major changes in precipitation, pressure and wind speed and direction across the globe.

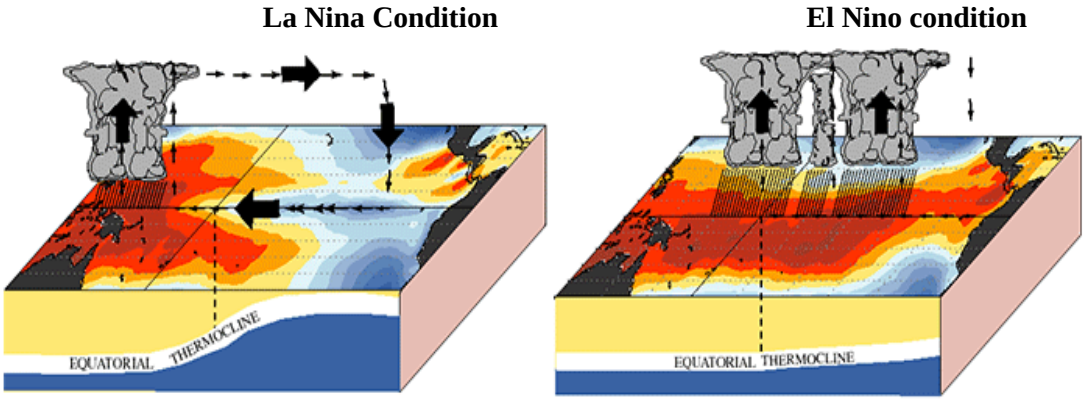

Figure 1.6 Schematic of ENSO cycle and precipitation variation. [http://meted.ucar.edu]

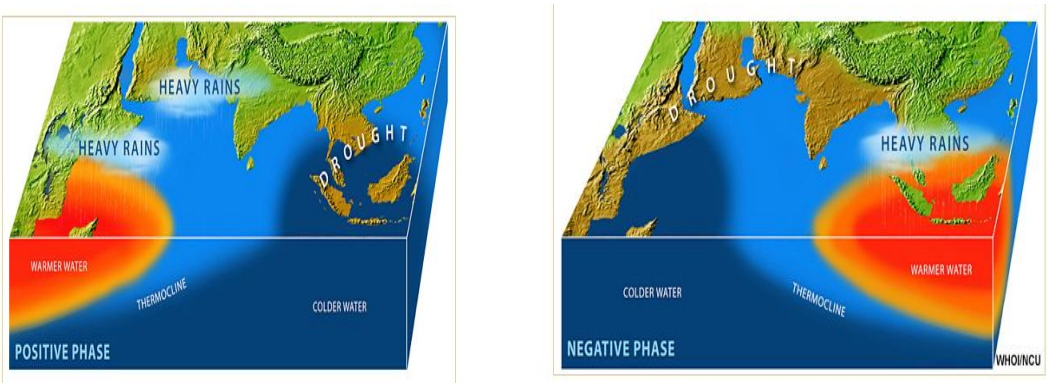

Figure 1.7 Schematic of IOD phases and precipitation over India. [http://meted.ucar.edu]

During El Nino events equatorial eastern and central Pacific Ocean have warmer than normal SST. Thermocline varies from west to east in Pacific Ocean. During El Nino event, energy transfers from warm western Pacific to comparatively cooler eastern Pacific. Deeper thermocline shifts from west to east in Pacific Ocean (fig. 1.6). At the end of El Nino event thermocline is shallower than normal everywhere in equatorial Pacific Ocean. Over shallow thermocline weak wind speed can also cause upwelling. The upwelling brings deeper cold water to the surface and reduces SST i.e. cooler water surfaces over eastern Pacific initializes La Nina event. During La Nina event strong easterlies allow water to accumulate over western Pacific Ocean which enhances precipitation near western Pacific land regions (Indian subcontinent).

Thermocline starts to deepen leading to suitable condition for El Nino event. Generally El Nino last for 12 to 15 months while La Nina for 1 to 3 years [www.meted.ucar.edu]. There are many indices that monitors the ENSO cycle effectively. One of the most widely used index is ONI (Oceanic Nino Index) which defines El Nino/ La Nina by tracking above or below normal equatorial Pacific SST variations. Nino Index has been calculated over four different regions named by Nino 1, Nino 2, Nino 3 and Nino 3.4.

The variability in the monsoons over India is also influenced by an east-west oscillation in SST anomalies in Indian Ocean. IOD is ratiocinated by Saji et al. (1999). They defined that the positive IOD phase is associated with colder eastern Indian Ocean, which strengthens trade winds over equatorial Indian Ocean and hence enhances rainfall over India (fig. 1.7). The negative phase of IOD decreases precipitation over Indian subcontinent. IOD event starts in May/June and spreads over equator ward in month of July/ August. Ajayamohan & Rao (2008) documented that IOD starts to diminish in September/October.

1.3 Research objectives:

Following by the research on different aspects of Indian summer monsoon, the present work focuses on the spatial and temporal distribution of rainfall over the west coast of India in association with orography and different ocean parameters during south west monsoon season. Below mentioned objectives have been addressed in this research.

I. Validation of remotely sensed TRMM 3B42 v7 rainfall data with *rain gauge* measurements (IMD Gridded Rainfall data set)
II. Spatial-temporal variability of rainfall due to orography of Western Ghats
III. Interlink of variations in adjacent oceanic parameters with rainfall variability over Western Ghats

1.4 Research questions:

To successfully conclude above research objectives, attempts have been made to investigate the following

I. How efficiently satellite rainfall estimates captures the *in- situ* rain records?
II. Which orographic feature enhances rainfall rate over WG? How rainfall distribution over WG changes with time and space?
III. Is it possible to relate the other monsoon system parameters (for example SST & WS) variability with raised precipitation rate over Western Ghats?

The outline of thesis is as follows. Chapter 2 gives theoretical background of the research theme. Specifications of study region and data procured are described in chapter 3. Chapter 4 describes the methodology adopted to analyse the research problems. In chapter 5, a detailed analysis of orographic rainfall patterns, topography, slope, elevation and spatial variation in heavy rainfall events with its connection to SST and WS has been discussed. The conclusion and recommendation are provided in chapter 6.

Chapter 2. Literature review

2.1 Indian summer monsoon over WG:

Spatial distribution of annual rainfall of India exhibits north-south oriented belt of heavy rainfall over WG. This capacious rainfall sustains the rich biodiversity and coastal ecosystem of the west coast of India. Forecasting accurate weather conditions over this undulating terrain is challenging task as it affects an efficient use of resources available to large population inhabited in WG. Basu (2005) compared day-1 to day-4 rainfall forecasts from numerical weather predicting models, National Centre for Medium Range Weather Forecasting (NCMRWF) and European Centre for Medium-Range Forecasts (ECMWF) over Indian region and reported that both of the models are able to predict the heavy rainfall rates over west coast of India in summer monsoon season but underestimates magnitude of heavy rainfall. Models introduce considerable systematic errors in forecasting rainfall over west coast ridgeline. Aforementioned study further reveals that ECMWF model which has included improved topographic definition depicts better heavy rainfall rates over WG. According to Bhowmik and Durai (2008), four different NWP models used by IMD for ISMR prediction up to 2 days (in year 2006) also underestimates orographic rainfall over WG. Above mentioned studies suggest that it is necessary to incorporate orographic feature influencing the south west monsoon rainfall over WG for better hazard management and prediction in future.

Patwardhan et al. (2000) observed that the irregular patterns of rainfall are in association with irregular terrain. Their study is based on 10 years of rain gauge measurements over funnel type gap of Ghats in Maharashtra state. Venkatesh & Jose (2007) indentified homogenous rainfall intensities in one of the coastal district and its adjoining areas in Karnataka using mean rainfall of 10-15 years obtained from rain gauges. Coextensive study carried out by Simon & Mohankumar (2004) to identify homogenous rainfall regions in Kerala, have also expressed the difficulty to relate topography with rainfall distribution. They have observed that some heighted apexes on windward side of WG in Kerala receive below normal rainfall. Raj & Azeez (2010) analysed 23 years of rainfall and observed that decreasing rainfall trend in Palakkad gap in WG near Kerala is mainly attributed to deforestation. Their study by correlating height and rainfall (from rain gauge stations) has further brought out the fact that the altitude, valley & hillock features give higher rainfall. Another extensive study carried out by Gadgil (2003), Francis & Gadgil (2005) addressed ISMR variations incorporating the propagation of TCZ, offshore convection, deep and large cloud systems over AS and ocean oscillations. Sarker (1966), U.S. De & Dutta (2005), Suprit and Shankar (2008) have developed models undertaking the different parameters to calculate rainfall over West coast of India. Grossman & Durran (1984), Ogura & Yoshizaki (1988) have discovered that WG's elevation is capable of deep convection well offshore in AS. An advanced study of Bookhagen & Burbank (2006) mentioned that relief can be used as an alternate for slope to study orographic rainfall in Himalayan region. They have used 5km×5km window to calculate relief and then studied variation of rainfall with relief and elevation in latitudinal direction using satellite data.

Francis & Gadgil (2005) suggested the need to study the trend of extreme rain events and mentioned that the intense rainfall events have tendency to occur at location 14°-16°N and near neighbouring locations of 19°N. They have further stated that extreme rain events are likely to occur near the orography. Rajeevan et al. (2008) analysed a strong coupling between inter annual and inter decadal variability of extreme rain events with SST, humidity and wind speed in the past 100 years of data set. Another extensive study has been carried out by Dash et al. (2009) which reflect different rainfall trends in the six different homogenous rainfall zones of India considering both duration and magnitude of rainfall to categorized different spells of rain events. They have presented the decreasing trend over peninsular region and west central region of India, which comprise of WG. Goswami et al. (2010) have also discovered decreasing trend of extreme rain events in the hilly terrain of North East Indian region. Their study further reveals that the topography of terrain is not influencing the variation in extreme rain events but it changes in out of phase with CAPE (convective available potential energy). Konwar et al. (2012) describes low and medium rain events fluctuate in accordance with variation in vertically integrated moisture transport (VIMT) and wind speed over AS and Bay of Bengal. The recent study by Rajendran et al. (2012) has predicted the forthcoming changes in rainfall distribution over WG focussing Karnataka and Kerala states, using IMD and MRI model data (20 km). Aforementioned study also addressed decreasing trend in moderate to heavy rainfall because of the warming of upper troposphere which consequently decreases lapse rate, vertical velocities, south westerly winds and moisture transport over WG. They have further stated that there will be decrement in the frequency of high to moderate rain events over windward side and increment over the lee side of WG in coming years. Most of the researches on extreme rain events have used mainly IMD 1°x1° gridded rainfall data and there is no documentation on extreme events focussing spatial distribution of frequency of extreme rain events over WG and its association with topography. The sparse coverage of the traditional rain gauges cannot provide essential information about the extreme rainfall in rugged terrain of WG (Bhowmik & Das, 2007). In a view of all above studies, to overcome gaps due to the lack of information and coarser resolution, as a part of advanced technology, the satellite rainfall data with high resolution of 0.25°x 0.25° has been utilized over WG and its adjacent oceanic region in the present work.

As per author's knowledge the earlier research work on Indian summer monsoon focussing west coast have emphasised variation in atmospheric parameters and orographical impact on rainfall pattern on regional scale (at state or district level) by enumerating data from rain gauge stations. Therefore in the present work orographical features (topography, elevation and slope) stimulating spatial and temporal variability of rainfall has been studied using very high resolution remotely sensed precipitation and elevation data over entire WG barrier.

2.2 Orographic precipitation:

Elliott & Shaffer (1962) have mentioned that the development of prediction processes and observation networks for accurate, short spell and quantitative precipitation forecast in mountainous areas is vital. They have analysed orographic precipitation on east-west oriented Santa Ynez mountain range, parallel to coastal California. Aforesaid study developed an

equation based on physical relationship between orographic precipitation, air mass properties, wind flow and terrain features for short term rainfall forecasting. Elliott & Hovind (1964) further preceded research on mountain barriers of southern California using rain gauge data and computed condensation and observed precipitation efficiency. Precipitation efficiency (PE) is a ratio of total precipitation rate to total condensation rate. Their study has concluded the PE is higher for convective activities and higher mountain produces more supersaturated water giving faster conversion rate hence induces heavy precipitation on windward side of the mountain. Marwitz (1980) utilized aircraft wind data, snowflakes samples and rate form rain gauge to study storms over San Juan's mountain range, Colorado, North America. The primary stage of storm is due to orographic blocking in stable atmosphere which leads to precipitation (Marwitz, 1980). In accordance with above result Jiang & Smith (2003) reasoned that in stable and non-convective atmosphere, snow generation and PE increases with the mountain width. As mountain width increases, it supplies adequate advection time for rain drop growth. Also as mountain width increases, slope decreases leading to less carryover of water droplets to the mountain peak. Therefore PE increases with mountain width. Carryover increases with a wind speed, so as wind speed increases PE decreases.

2.3 Indian summer monsoon over WG using TRMM datasets:

Over a land region, rain gauges are most reliable and trusted instruments for rainfall mapping. But some of the remote regions over land are inaccessible i.e. mountainous terrain therefore radar or in situ measurements over such an area are difficult to record. Satellite rainfall estimations are beneficial over such a region for better analysis of spatial and temporal rainfall variability. In the era of satellites, TRMM has first onboard precipitation radar which enhances the microwave rainfall estimations over land as well as over ocean. However it has been detected by myriad researchers that satellite measurements have some biases in rain rate compared to the rain gauge measurements. Mitra et al. (2009) observed that the satellite rainfall data is practicable but still requires calibration at regional scale. TRMM daily rainfall algorithm is able to detect spatial pattern of rainfall noticeably over Indian region in year 2006 while heavy rainfall intensities are found to be underestimated over west coast of India (Mitra et al., 2009). To overcome the limitation of TRMM data, Mitra et al. (2009) have proposed new daily data sets NMSG i.e. daily merged rain gauges (400) readings with TRMM satellite rain rate which enhances the satellite rainfall product. Mitra et al. (2013) have extended their previous work to compare daily TRMM3B42v6 rainfall and IMD data sets for 14 seasons (year 1998 to 2011). Their analysis on 14 years TRMM3B42v6 rainfall data sets unfolds that rain gauge is able to capture warm rain over WG while daily TRMM estimates underestimates the heavy orographic precipitation as it is not sensitive to warm rain detection. Nair et al. (2009) compared orographic rainfall estimated by TRMM 3B42v6 satellite daily product and IMD rainfall data over Maharashtra state. Based on their research, TRMM measurements are consistent on seasonal, monthly and daily scales but orographic heavy precipitation is unsatisfactorily captured by TRMM over respective study regions. It is further concluded by Nair et al. (2009) that in daily rainfall data sets the lower rainfall is overestimated and higher rainfall is underestimated by satellite but correlation between TRMM and IMD rainfall at monthly and

seasonal scale is acceptable. The elaborative study of daily and seasonal variability of Indian summer monsoon is carried out by Rahman et al. (2009) over Indian region using TRMM, GPCP and IMD rainfall data. They observed high summer monsoon (JJAS months) rain over WG and Himalayan foothills is captured well by TRMM data. Even though TRMM depicts correct phase of intraseasonal variations accurately with that of IMD, it underestimates mean seasonal variability in rainfall over Indian region. The large standard deviation (SD) in seasonal rainfall amount noted by IMD daily rain records from year 1998 to 2003 is well captured by TRMM daily rainfall data. Rahman et al. (2009) defined a box over west coast (19.5-23.5N, 72.5-86.5E), and observed that over this region the seasonal (JJAS) mean rainfall is 7.4 mm/day recorded by IMD data while it is 6.4 mm/day by TRMM 3B42 and SD from IMD record is 13.8 mm/day while SD from TRMM 3B42 is 13.5 mm/day for 6 years (1998-2003). Therefore according to Rahman et al. (2009), TRMM rainfall estimates are realistic enough to be used for synoptic and longer time scale analysis of ISMR.

2.4 Association of rainfall over WG with SST and WS over AS, ENSO cycle and IOD:

Izumo et al. (2008) have mentioned the need to understand the underlying mechanism of SST fluctuations that controls variability of rainfall intensity. Shukla (1975) evaluated physical mechanism between AS SST, WS, moisture flux and ISMR. Aforementioned research explained that the reduction in monsoon rainfall amount is related to the weak WS over western AS and cold SST, which is attributed to reduced sea level pressure and therefore less evaporation over AS**.** Shukla & Mishra (1977) studied the lead-lag relationship between SST and WS over AS affecting monsoon rainfall over central and western India. Their study found out significant positive correlation between AS SST of July with August rainfall over central and western India. The correlation between WS and rain is positive for the same month and negative for the lagging month. They suggested that the increase in WS increases the evaporation and upwelling in AS which leads to decrease in SST. Colder SST anomalies tend to reduce precipitation over India in subsequent months. The study of Izumo et al. (2008) has provided the new methods for better forecast of Indian summer monsoon considering regional scale as well as ENSO cycles. Their study concludes that upwelling at Somalia coast maximizes during summer monsoon season because of south west winds. Due to upwelling, SST tends to attain below normal values at Somalia coast and warm water shifts towards the eastern AS. This acts as a main moisture source for ISMR. Further Izumo et al. (2008) observed that increased upwelling at Somalis coast limits the westward extent of warm pool (SST>28^{o}C) hence decreasing rainfall at west coast of India. This is due to less evaporation and insufficient moisture transport towards WG. The alongshore variability in wind velocities over western AS affects the upwelling at Somalia coast hence the intensity of rainfall over west coast of India. A strong upwelling takes place in western AS due to increased wind speed. This restricts the extent of warm pool in AS and hence the amount of moisture transport towards west coast of India. Nino 3.4 SST of previous year affects the ISMR in the next season but IOD doesn't influence the following summer monsoon at west coast of India. A positive lag-correlation is observed between previous winter ENSO conditions and the subsequent Indian summer monsoon (Imuzo et al, 2008). Imuzo et al. (2008) also extended their work to analyse monthly

variations in rainfall over West coast due to SST and WS over AS and mentioned that in June, rainfall intensity is dependent on SST as well as on WS variation. In July and August as SST drops down rainfall is controlled by upwelling at Somalis coast. They have declared that for better monsoon forecast not only large scale circulations but also accurate estimation of AS local forcing need to be studied. Krishnmurthy & Kirtman (2002) have summarised that most of the researches focussing relationship between ISMR and AS SST, Indian Ocean SST, WS, ENSO cycle. Rao & Goswami (1988) observed above normal SST over Indian Ocean in preceding months induce increment in summer monsoon rainfall. Krishnmurthy & Kirtman (2002) showed weak positive correlation between Indian Ocean in MAM months with that of JJA summer monsoon rainfall over India, whereas there is no significant correlation between Indian Ocean SST and monsoon rainfall in JJA. Further their study disclosed the fact that above normal rainfall in JJA months results in cooling of AS. Clark et al. (2000) focused the variation in Arabian and Indian Ocean with JJAS rainfall over India. They have stated that JJAS rainfall over Indian subcontinent has weak positive correlation with the northern Arabian SST of past DJF months and strong positive correlation with SST of central Indian Ocean in past SON months. Further their study evaluated relation of ISMR with ENSO and end up with moderate connection of ENSO and ISMR. But ISMR is not solely controlled by ENSO. Krishnamurthy & Kinter (2002) have listed some imperative studies that explain the apparent shift in the Walker circulation affects the local Halley cell circulation over monsoon region of India during El Nino events. This reduces rainfall of summer monsoon season. Saji et al. (1999) have discovered inherent air-sea interaction in Indian Ocean independent of ENSO cycle, which impacts monsoon precipitation. This SST gradient between tropical western and south eastern Indian Ocean is named as Indian Ocean Dipole (IOD) which can be monitored using Dipole mode Index (DMI). DMI modulates the trade winds and hence the rainfall anomalies over India subcontinent, Indonesia and Africa. But no significant correlation is identified by Saji et al. (1999) between IOD and rainfall intensity over India. In a context of extreme rainfall events in Indian summer monsoon and IOD, Ajayamohan & Rao (2008) mentioned significant negative correlation between number of extreme rainfall events (R>100mm/day) over central India and cold SST anomaly of IOD. In their study cold SST anomaly of south eastern Indian Ocean is considered as an IOD event. The reason for increasing extreme rainfall events over central India is related with frequent IOD events due to warming environment. Further to this, no association has been found out in ENSO variations and number of extreme events by Ajayamohan & Rao (2008).

Chapter 3. Study area and data utilized

3.1 Study area

The WG is a chain of highlands running along the western edge of the Indian subcontinent, from the states Maharashtra, Goa, Karnataka and Kerala. The study is focused on region experiencing orographic rainfall bounded between latitude 8° to 21° N and longitude 70° to 78° E, as illustrated in fig.3.1. It has been observed from DEM data that the WG runs parallel to West coast of India 50 km away on an average from shore line. WG extends about 1600 km (North-south) in length and 100km (East-West) in width (Dept. of biotechnology Gov. of India & Dept. of Space Gov. of India, 2002). The average elevation of WG is approximately 800 m with some apexes race more than 2000 m elevation. To analyse change in SST and WS, the AS (58° to 75°E and 0° to 20°N) and Indian Ocean (30° to 120°E, -40° to 39°N) has been taken into consideration.

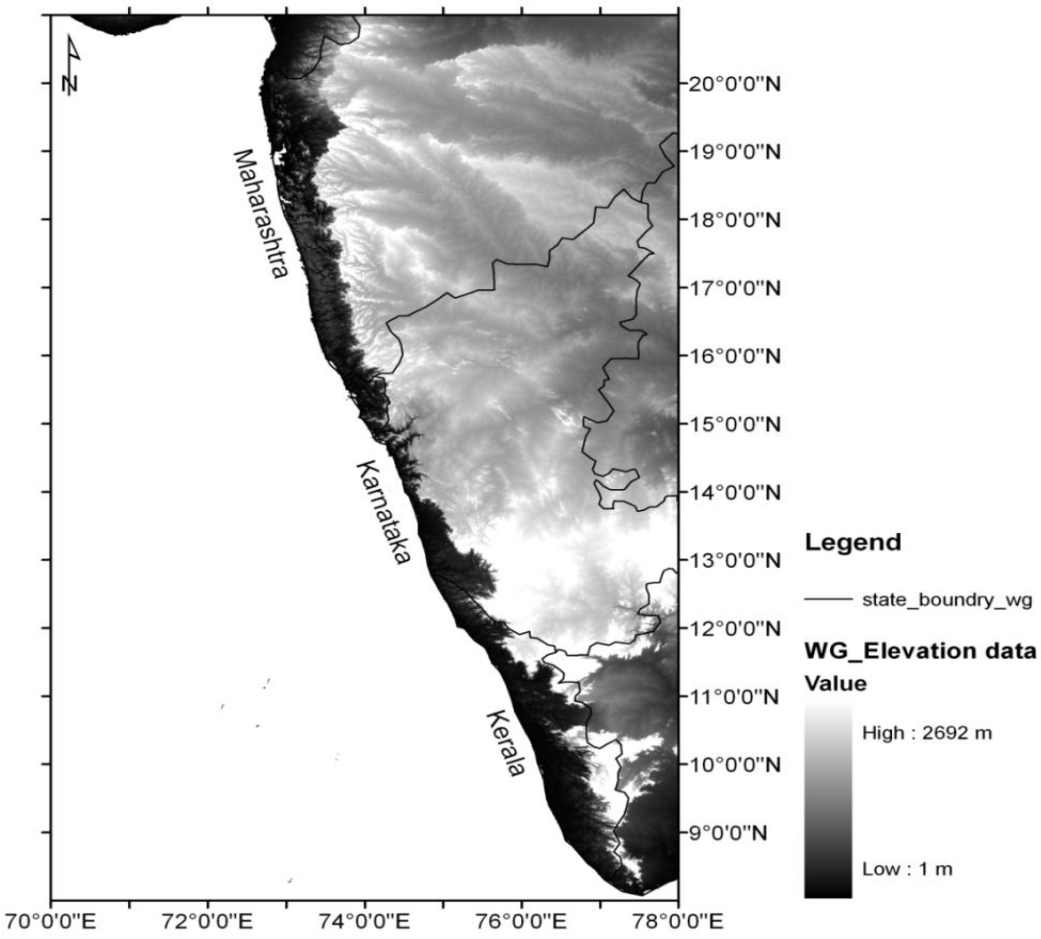

Figure 3.1 Study region of WG (8-21°N, 70-78°E)

3.2 Data utilized:

- ***In situ data:***

3.2.1 IMD rainfall data:

The IMD 0.5° gridded daily data from year 1998 to 2005 has been utilized in the present study. The IMD gridded data is available from year 1971 to 2005. This gridded data has been developed by IMD over Indian region using weighted interpolation technique on rain gauge observations. The data set is well validated and reliable (Rajeevan & Bhate, 2009). The starting point of this gridded data is 6.5°N and 66.5°E with total (69x65) grid points. Also some selective IMD station (rain gauge) data for extreme rainfall events have been used in the present study.

- ***Satellite products:***

3.2.2 TRMM 3B42 v7 rainfall:

Newly released TRMM (Tropical Rainfall Measuring Mission) 3B42 version 7 rainfall data has been utilized to study the variation of precipitation over WG of Indian subcontinent. TRMM TMI passive microwave sensor measures minute amount of microwave energy emitted by Earth and atmosphere. It observes water vapour, cloud water and rainfall intensities. It has additional low frequency channel which records high rain rate in tropics. TRMM PR (Precipitation Radar) retrievals are also used to calibrate TMI (TRMM Microwave Imager) rainfall. TRMM 3B42 v7 daily rainfall (mm/hr) data is available with fine resolution i.e. 0.25°x0.25° granule size. In TRMM 3B42 v7, 3hourly IR estimations are merged and then the rain gauge data are used to correct a large-scale biasing to the 3B42 algorithm over land [http://trmm.gsfc.nasa.gov/3b42.html]. TRMM 3B42 v7 rainfall data is available on NASA's web link. Rainfall data of Indian summer monsoon months (JJAS) for 15 years (1998 to 2012) have procured and studied for orographic as well as extreme rain events.

3.2.3 ASTER GDEM:

To study orographical aspects, ASTER digital elevation model data is acquired from [http://www.jspacesystems.or.jp/ersdac/GDEM/E/4.html]. The ASTER (Advanced Space borne Thermal Emission and Reflection Radiometer) DEM data is georeferenced to WGS-84 datum and Universal Transverse Mercator projection. The ASTER data is available at 30 meter resolution with 1x1 degree tiles. The estimated accuracies for ASTER DEM global product is 20 meters for vertical data and 30 meters for horizontal data at 95 % confidence.

3.2.4 KALPANA-1 SST:

ISRO launched KALPANA-1 satellite in year 2002 in geostationary orbit and positioned at 74°E. KALPANA-1 has onboard a VHRR (very high resolution radiometer) sensor with 3 channels; visible (resolution: 2km), water vapour (resolution:8 km), thermal IR (resolution:8km). VHRR measures SST through its thermal IR channel. 10.5 to 12.5 micrometer thermal IR channel is used for SST retrieval because sea surface emissivity at this wavelength

reaches up to 0.95 and atmosphere is considerably transparent. IR signals are attenuated by intervening atmosphere between their paths from sea surface to satellite sensor. Therefore algorithm is developed for KALPANA-1 SST which takes into account water vapour concentration and solar zenith angle as well as buoys SST readings (Shahi, et al., 2011). KALPANA-1 SST is available from year 2008. Therefore KALPANA-1daily SST data has been observed from year 2008 to 2012. KALPANA-1 SST data for year 2008 and 2009 is available with resolution of 0.5° and covers region between -50° to 50°N, 30° to 120°E. While 2010 onwards the SST data has refined to 0.1°resolution bounded between -40° to 40°N, 30° to 120°E. KALPANA-1 data has been gathered from [http://www.mosdac. gov.in/login.jsp].

3.2.5 Windsat wind speed data:

10 meter surface wind data is available from Windsat polarimetric radiometer on aboard Coriolis satellite. It provides WS at low frequency, medium frequency and all weather conditions. Windsat data is available from year 2003 onwards on the data portal of Remote Sensing System (California) [www.ssmi.com]. Data comes with granule size of 0.25°x0.25°. All weather surface WS is available only from Windsat data (7^{th} band), which is very useful to supply WS even in rainy conditions. Windsat provides global data in -90° to 90°N and 0° to 360°E region. The mathematical equation to convert the satellite recorded digital counts (or digital numbers: DN) into WS is as follows

$$All\ weather\ WS\ (m/s) = DN\ value \times 0.2 \quad (3.1)$$

DN values: 0 to 250= Valid geophysical data

251= Missing data

252= Sea ice

253= Observations exist, but are bad (i.e. sun glint)

254= No observation (near land 75km in rain, 50 km in no rain)

255= Land mass

The WS between the ranges 0 - 50 m/sec can be retrieved from WINDSAT satellite.

3.2.6 OI TMI SST:

The TRMM Microwave Imager (TMI) carried on NASA's TRMM satellite is a microwave radiometer capable of retrieving SST in cloudy conditions. Global SST data is available from latitudes 40°S to 40°N, with spatial resolution of 0.25°. TMI SST daily data is available at ascending-descending paths. Therefore there are some gaps in the global SST data. TMI covers most of the AS region in one of its ascending path. To fill these data gaps Remote Sensing System (California) provides microwave daily OI (optimally interpolated) SST data [www.ssmi.com]. TMI SST algorithm removes roughness of the sea. OI product takes care of day and night time SST fluctuations. OI SST is an improved version of SST data since it incorporates the buoys data to estimate and normalize the errors and contaminated rain, cloud pixels. It also estimates new SST for the day even if there is no new SST observation for the respective day i.e. from previous days SST observations. Below mentioned expression is used to convert the satellite recorded digital counts (or digital numbers: DN) into SST data in (°C)

$$SST\ (°C) = [DN\ value \times 0.15] - 3 \quad (3.2)$$

DN value: 0 to 250= valid SST

251= Missing data

252=sea ice

253,254=missing data

255= land

TMI can resolve SST values ranging between -3°C to 34.5°C.

3.2.7 Nino 3.4 Index:

Nino3.4 index is a measure of monitoring and prediction of ENSO cycle which modulates SST, sea level pressure, precipitations especially over equatorial pacific region. Nino 3.4 index is based on deviation of equatorial Pacific ocean SST to its long term average, bounded between 5°S-5°N and 170°W-120°W region. Refer fig.3.2, Nino 3.4 index has unit in degree centigrade. This index can be used to study El Nino and La Nina effect i.e. global influence on summer monsoon season over Indian sub continent due to variations in equatorial Pacific Ocean. Monthly Nino 3.4 index is available on NOAA's climate prediction center [www.cpc.ncep .noaa.gov/data/ indices] from year 1950 to 2013.

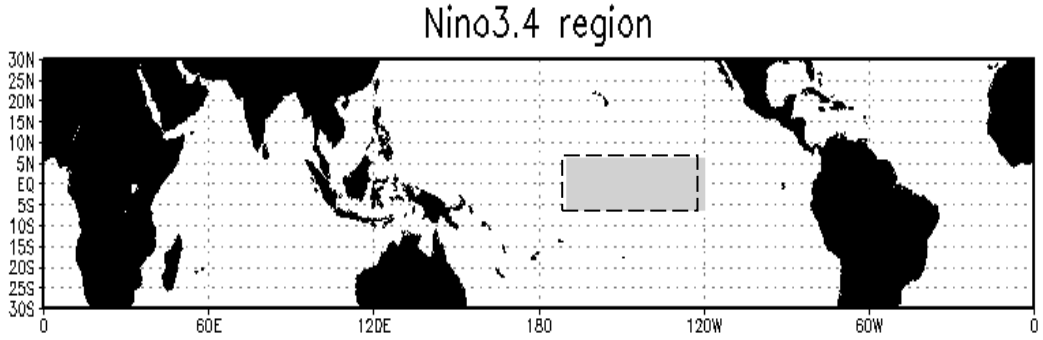

Figure 3.2 Nino 3.4 region (5°S-5°N and 170°W-120°W) in Pacific ocean. [http://www.esrl.noaa.gov/]

3.2.8 Dipole Mode Index (DMI):

As shown in fig.3.3, DMI is SST gradient between western equatorial Indian Ocean (IO) and south eastern equatorial IO. i.e.

DMI= SST [50°-70°E, 10°S-10°N] – SST [90°-110°E, 10°S-0°N] (3.3)

DMI is given in units of degree centigrade. This gradient is also known as Indian Ocean dipole (IOD). Monthly DMI is available from year 1958 to 2010. The data is accessible at web site: [www.jamstec.go.jp/frcgc/research/d1/iod/HTML/Dipole%20Mode%20Index .html] .

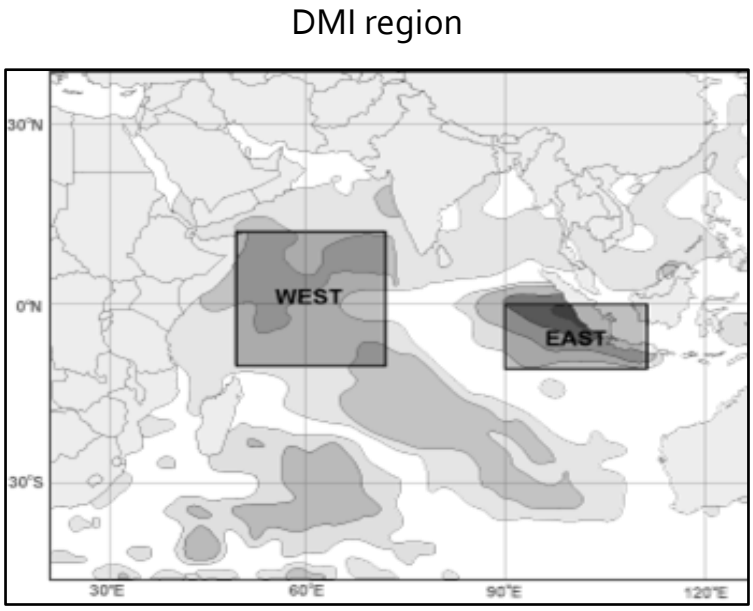

Figure 3.3 Dipole mode index region in Indian Ocean [http://www.bom.gov.au/]

3.3 Data analysis:

3.3.1 Validation of TRMM 3B42 v7

TRMM 3B42 v7 rainfall data has been launched by NASA in June 2012. It includes reprocessed data for AMSU microwave estimations. AMSR-E data, which was used in all previous versions of TRMM 3B42, ceased producing data as its antenna stopped rotating in Oct. 2011. After launching of TRMM 3B42 v7 data in June 2012 one more processing anomaly in rainfall data over oceans had been identified by TRMM scientific group. The new improved data over ocean is then reloaded by respective data suppliers in Jan. 2013. Therefore it has become mandatory to check the validity of this new version for accuracy of further research work. Fig. 3.4 describes the flowchart for validation of TRMM 3B42 v7 rainfall with IMD gridded rainfall data.

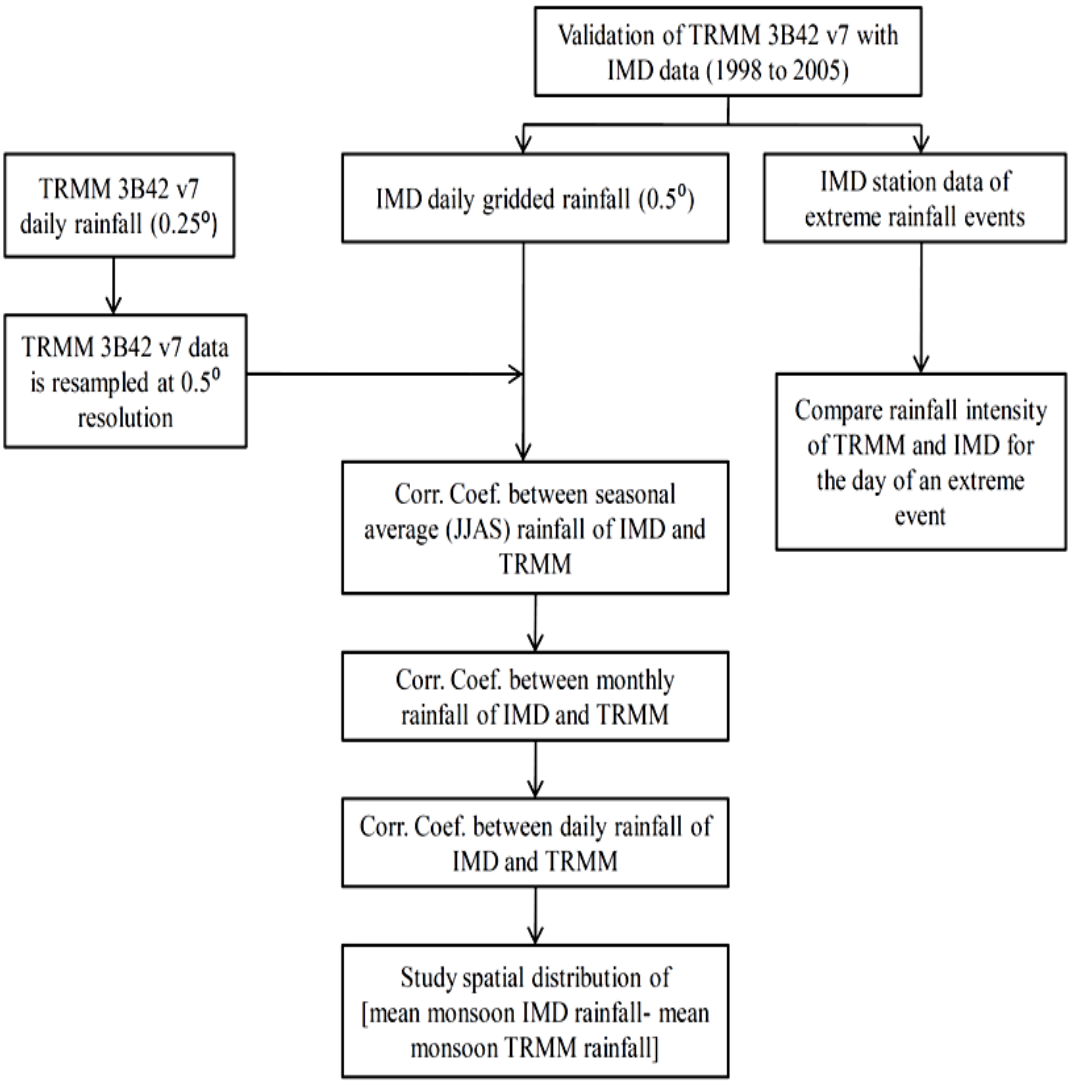

Figure 3.4 Flowchart for the validation of TRMM data with IMD data

Validation of TRMM 3B42 v7 rainfall with IMD rainfall records has been done by observing seasonal average as well as individual months average. The analysis has been carried for all years from 1998 to 2005. For the validation purpose the TRMM data has been scaled up to 0.5°. The comparative analysis for the mean monsoon rainfall between IMD data and TRMM 3B42 v7 estimates over each spatial location of WG (459 points) for 1998 (above normal rainfall year) and 2002 (drought year) is depicted in Figure 3.5 (a & b). Our analysis reveals that the mean monsoon rainfall estimates from these two different sources found to be strongly correlated for the period 1998-2004 (varies from 0.82 to 0.88). All correlations are found to be significant at 1% significance level for all the spatial location (spaced every 50 km) of WG.

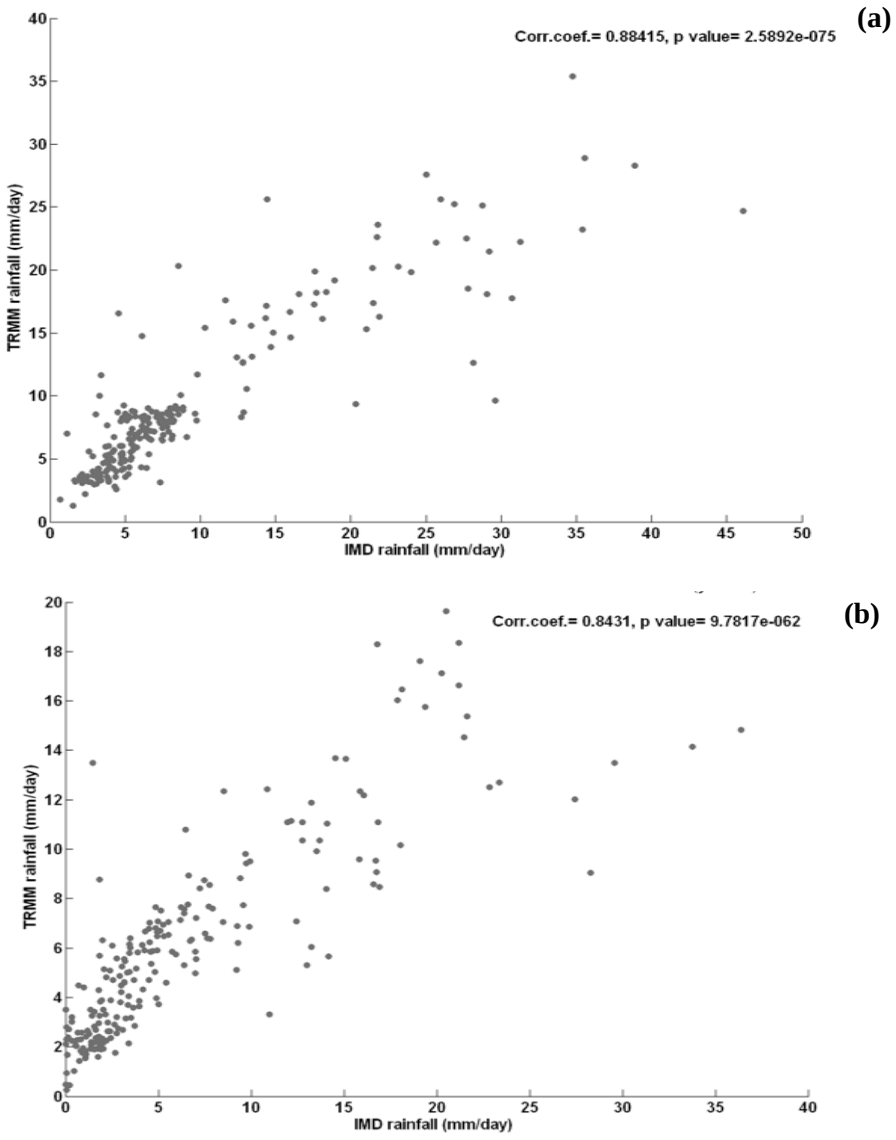

Figure 3.5 Scatter plot of TRMM 3B42 v7 and IMD seasonal averaged rainfall (mm/day) over WG with correlation coefficient. a) for year 1998 b) for year 2002

Correlation between IMD rainfall and TRMM 3B42 V7 rainfall data for individual summer monsoon months varies between 0.60 to 0.88 (except for 2005). These monthly correlations for 459 points over WG are significant at 1% significance level. It is worth mentioning here that (please refer fig. 3.6a & 3.6b) in June and July the correlation between IMD and TRMM 3B42 v7 rainfall over entire WG is maximum and it steps down in the month of September. Similar results are also documented by Nair et al. (2009) over Maharashtra using TRMM 3B42 v6 rainfall data set.

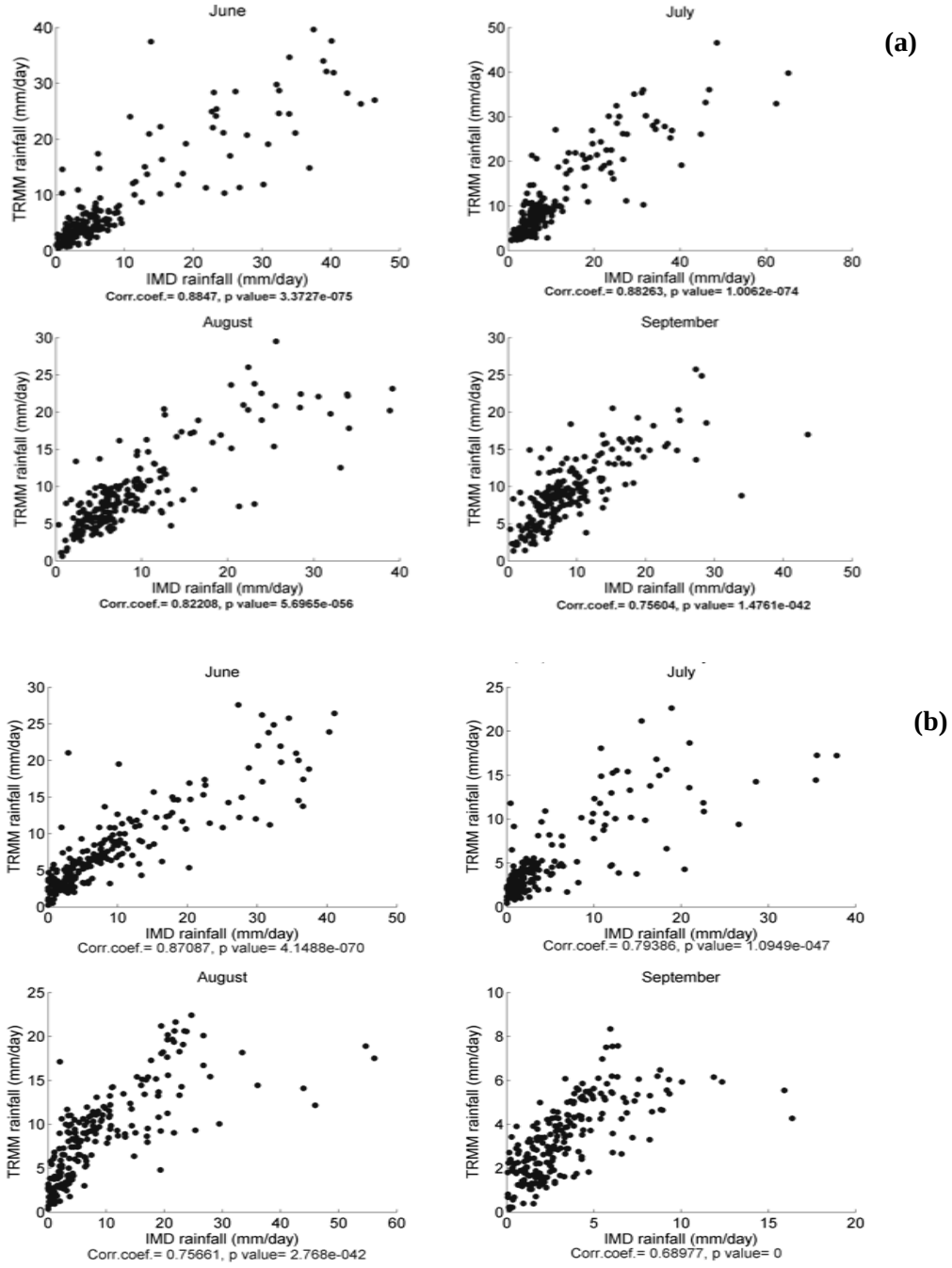

Figure 3.6 Scatter plot of TRMM 3B42 v7 and IMD monthly averaged rainfall (mm/day) over WG with correlation coefficients at the bottom of every plot. a) for year 1998 b) for year 2002.

The daily rainfall correlation of TRMM 3B42 v7 rainfall data with IMD rainfall data is found to be less compared to monthly and seasonally averaged correlations. It ranges between values 0.23 to 0.46. This correlation for the 56,000 points (122 days and 459 spatial locations in WG) is significant at 1% significant level. The scatter plot (fig. is not shown here) interprets that TRMM 3B42 v7 satellite data overestimates low rain rates and underestimates high rain rates.

This has also been reported by Nair et al (2009) for TRMM 3B42 v6. Fig. 3.7 depicts the spatial pattern of seasonal rainfall (composite for year 1998 to 2005) from IMD gridded data, TRMM 3B42 v7 data and the bias between the two data sets. The rainfall bias at each spatial location for seasonal mean rainfall is calculated using the following expression.

$$\text{Rainfall bias} = \text{spatial pattern of (IMD rainfall- TRMM 3B42 rainfall)} \qquad (3.4)$$

It has been observed that spatial pattern of seasonal averaged rainfall of IMD is well captured by TRMM satellite; however TRMM 3B42 v7 underestimates rainfall intensity especially over orographic region. Both of the IMD and TRMM rainfall data sets reveal that the highest rainfall are located between 13-14°N and 74-75°E. The rainfall bias over windward side of the WG has positive values (i.e. IMD rainfall is greater than satellite recorded rainfall for same location) while lee ward side of the WG has negative rainfall bias value. The averaged bias in rainfall intensity over entire study region in JJAS months is approximately 0.5 mm/day. Overall it has been observed that TRMM 3B42 v7 daily rainfall is more or less obeying IMD daily rain records.

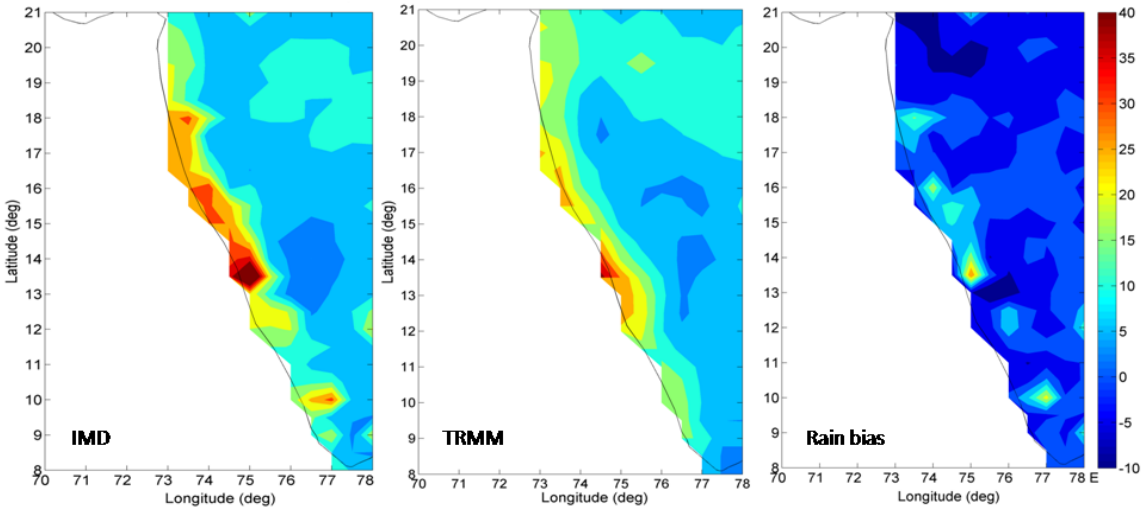

Figure 3.7 Spatial distribution of seasonal mean rainfall over WG using IMD and TRMM data and rainfall bias between both the data sets. Colour bar indicates the rainfall in mm/day.

Further to this, the TRMM 3B42 v7 rain estimates were compared with the rain gauge station data for some of the very high rainfall records (based on IMD reports) over different locations. Statistical information of rain records provided in Table 3.1 reveals that TRMM 3B42 v7 daily rainfall data does not pick the intensity of extreme rainfall events accurately. Present analysis also shows that the TRMM 3B42 v7 underestimated the rainfall intensity of extreme rainfall event on 25th July 2006 but it captures rain gauge rainfall pattern for the same event.

Table 3.1 IMD rain gauge records and TRMM 3B42 v7 rainfall for same day

Date	Lat	Long	Place	IMD (mm/day)	TRMM3B42v7 (mm/day)
25/07/2006	19.0N	73.0E	Maharashtra	34.4	32.0
26/07/2006				720.0	380.3
27/07/2006				52.0	68.0
29/09/2010	18.5N	73.8E	Maharashtra	60.0	54.0
04/10/2010	18.5N	73.8E	Maharashtra	166.0	99.4

According to above mentioned results, seasonal and monthly rainfall rates of TRMM 3B42 v7 over WG are in accordance with IMD rainfall records, however, overestimation/ underestimation of daily rainfall as compared to rain gauge based IMD measurements have been observed over this mountainous terrain. Therefore, for better accuracy, present analysis is based on the annual and monthly rainfall estimations generated from TRMM 3B42 v7.

3.3.2 Comparison of CARTOSAT DEM and ASTER GDEM

In order to resolve orographic features over WG, CARTOSAT Digital Elevation Model (CARTO DEM) has been used. However CARTOSAT DEM is available with finest resolution (2.5m), but it has been observed that elevation over WG could not be resolved accurately by CARTOSAT DEM. Some negative values in CARTOSAT DEM were found over coastal area unlike ASTER GDEM. The elevation at 12.86 N, 75.03E (location at coastal Karnataka) is about – 66 m as per CARTODEM, whereas the elevation at this location is approximately 24 m from ASTER GDEM. Therefore, ASTER GDEM found to be more appropriate to evaluate the elevation and topography of WG. It also has been observed that CARTODEM has some missing /null elevation values in dataset (refer fig. 3.8). The maximum elevation over WG, which could be resolved by CARTODEM is about 1750 m, whereas ASTER data shows that maximum elevation over WG is 2281 m which is approximately close to the highest peak in Western Ghats i.e. 2695m (surveyed by Western Ghats Ecology Expert Panel, 2011) in Kerala region. Considering the above mentioned limitations in CARTODEM, we preferred to use ASTER GDEM data for the present research work.

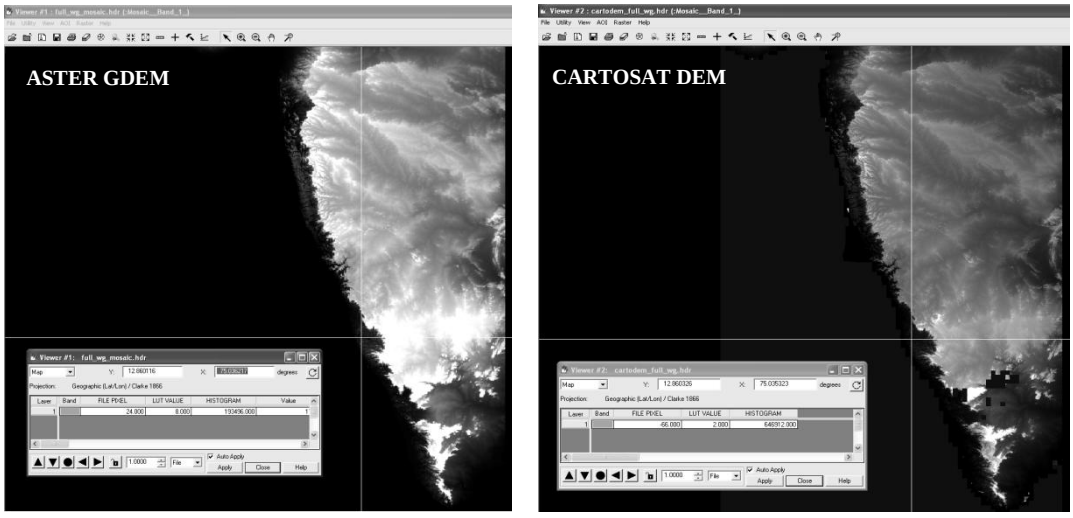

Figure 3.8 Elevation data in meters. The statistical information of DEM is analysed in ERDAS image processing software. The box below shows elevation at (75.03°E, 12.86°N) a) ASTER GDEM shows elevation at point is 24 m; b) CARTOSAT DEM shows the elevation at point is -66m & some null data pixels.

3.3.3 Comparison of KALPANA-1, TMI SST

KALPANA-1 SST data for year 2008 and 2009 has poor resolution (50 km) and quality (the spatial pattern of SST variation could not be captured) as compared to TMI SST data (resolution is 10 km). KALPANA-1 SST for year 2010 to 2012 is informative with finer resolution of 0.1 degree and has considerable correlation with TMI SST data (Shahi et al., 2011) after slight bias correction. In KALPANA-1 'daily' SST data sets, the SST values are found to be missing due to cloud covers over oceanic region, near west coast of India and also the daily SST data set of KALPANA-1 is not continuous. This leads to ambiguity in the interpretation of influence of SST variation on intensity of rainfall. For better accuracy, MODIS and TMI SST daily data sets have also been analysed but both of the satellites have missing values in daily data sets i.e. cloud cover in MODIS images and only ascending path coverage of TRMM-TMI over AS. TMI daily SST data is available for all weather conditions in ascending and descending paths but entire AS is not covered by the ascending and descending paths of the TMI. To overcome the issue of data gaps, one more SST estimate OI (optimally interpolated) daily SST (0.25° resolution) based on TMI SST is used in the present study. In addition to this, comparison has been done between correlation coefficients of TMI SST–rain (over WG) and KALPANA-1 SST-rain (over WG). Daily SST data from KALPANA-1 found to be negatively correlated with TRMM 3B42 rain estimates for years 2010 to 2012, which is not in concurrence with the previous research on Indian summer monsoon. Also the correlation between KALPANA-1SST and rain was not significant. This may be an artefact of missing daily SST observations and cloud cover over eastern AS during South-West monsoon. Considering all above mentioned facts, KALPANA-1 daily SST has been discarded to study the extreme rain events. Therefore for daily SST analysis OI TMI product by Remote Sensing System has been used.

Chapter 4. Methodologies to characterize orographic precipitation

4.1 Orographic precipitation over WG:

Firstly the orographic influence on spatial and temporal variability of rainfall at 25 km grid size has been investigated as a function of topography of WG of India. For this purpose the ASTER GDEM (flowchart is given in fig. 4.1) and slope data sets have been procured & resampled from 30m to 25 km resolution over the study region.

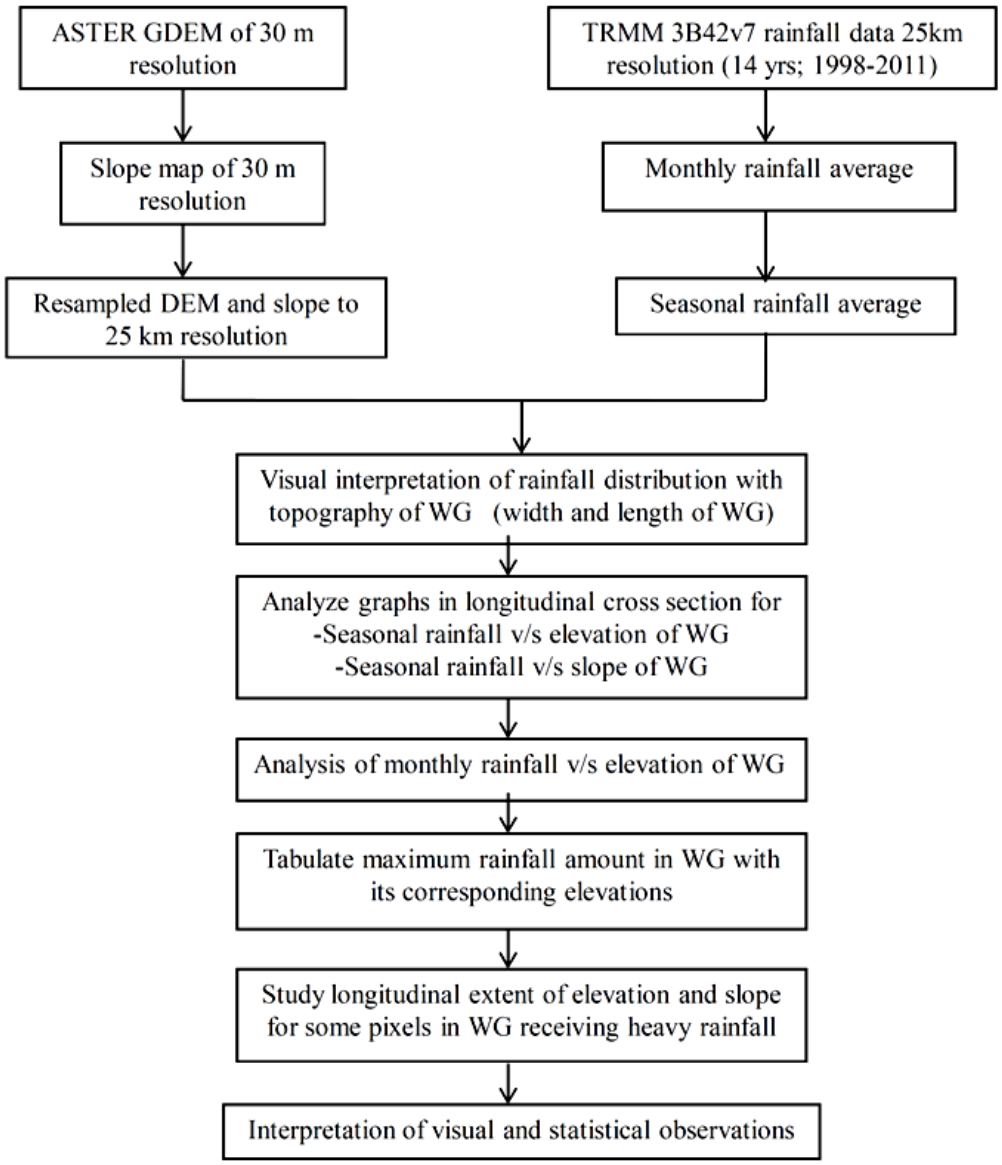

Figure 4.1 Flowchart indicating steps carried out to investigate variation in orographic rainfall over WG

After resampling, small variations in elevation, slope has been smoothened out and prominent values stood out. A variation of topography, altitude and slope of WG are examined using DEM data, slope map and topographic information. TRMM rainfall estimates over ocean are masked before statistically analysing orographic rainfall over WG with respect to height & slope data. It has been very crucial to demark boundary of WG considering its parts in every states. According to report of Western Ghats Ecology Expert panel (2011), WG boundary is defined by mapping forest/vegetated area with certain altitude. Eastern edge is delimited with forest cover above altitude 500m while western edge consist of forest cover above 150m elevation. Consorting with this report, in the present work elevation exceeding 600m is considered as a WG mountain barrier; so that prominently elevated features of WG could stand apart.

Further to identify heavy rain events, the rainfall data over study has been classified in to different rainfall regimes depending on magnitude of rainfall. Most of the studies on extreme events over India (Goswami et al.,2006; Rajeevan et al.,2008; Goswami et al.,2010; Konwar et al.,2012) describe high rainfall events of rainfall rate (R) >100 mm/day and very high rainfall events with intensity R>150 mm/day. For, the quantitative estimation of threshold for extreme rainfall events, the histogram/ probability distribution function for daily rainfall during principal rainy season has been generated for both IMD and TRMM 3B42 v7data sets (fig. 4.2 & 4.3). An extreme rainfall event may be described as a rare to rarest event (i.e. the event which lies toward the tail of the rainfall probability distribution), having the minimum probability of occurrence. To identify the threshold of extreme event the intensity corresponding to 99.5 & 99.75 percentile of the data set has been examined. According to the IMD rainfall records, the 99.5 percentile is equivalent to 149.06 mm/day rain rate whereas 119.57 mm/day is the 99.5^{th} percentile of the TRMM 3B42 v7 rain measurements (underestimates as compared to IMD data). Similarly, 99.75^{th} percentile of the TRMM 3B42 v7 rainfall data is 150.05 mm/day while it is 179.55 mm/day for IMD rainfall data. Therefore these two thresholds (150>R>120 mm/day & R> 150 mm/day) have been set for TRMM 3B42 v7 daily rainfall data over WG to parameterize the number of extreme rain events.

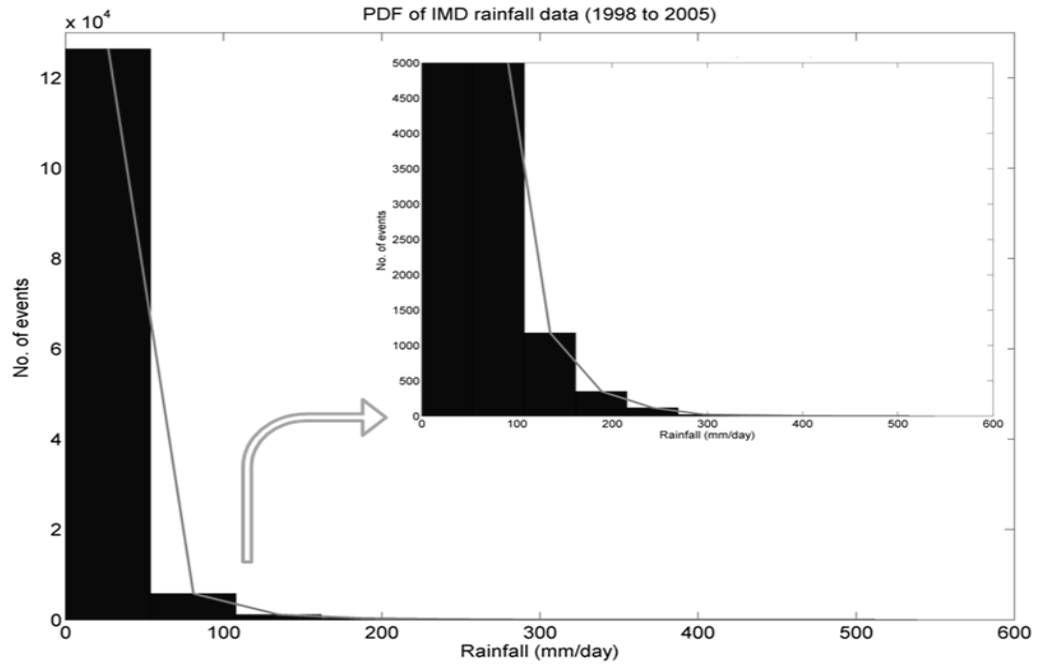

Figure 4.2 PDF of IMD daily rainfall data of 0.5° resolution over WG from 1998 to 2005. X axis represents rainfall (mm/day). Y axis indicates number of events corresponding to the rainfall intensity.

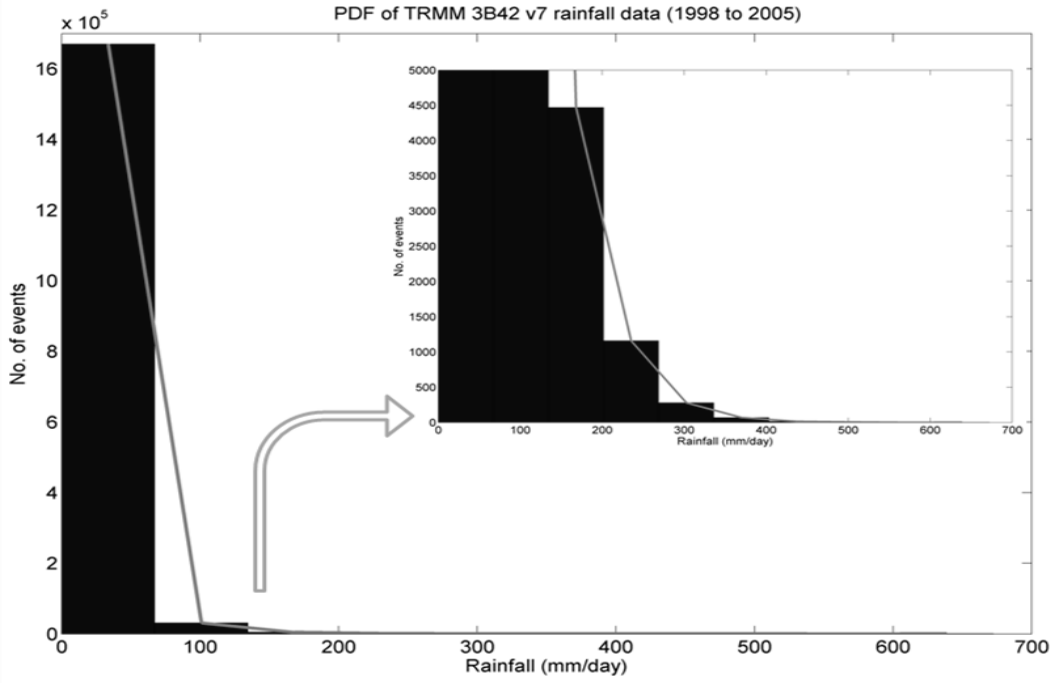

Figure 4.3 PDF of TRMM daily rainfall data of 0.25° resolution over WG from 1998 to 2005. X axis represents rainfall (mm/day). Y axis indicates number of events corresponding to the rainfall intensity.

4.2 SST, WS, OLR variations with rainfall

4.2.1 Inter annual variations

The association of variation in SST, WS over AS with the intensity of downpour over mountainous terrain of WG have been studied using satellite estimates of SST and WS. For the analysis of SST variation at monthly and annual scale, KALPANA-1 SST data has been utilized. Monthly SST average is calculated from daily KALPANA-1 SST data for the 4 months of principal rainy season (JJAS). While calculating monthly or yearly SST averages from daily SST data sets the missing data files as well as missing SST pixels due to cloud cover have been taken into care. First the variations in SST and WS (30° to 120°E & -40° to 39°N) in summer monsoon season have been analysed using visual interpretation method to understand the mechanism of monsoon circulation. Figure 4.4 displays the flowchart for above mentioned analysis.

To establish the relationship of the monsoon parameters i.e. AS SST and WS (58°-75°E & 0°-20°N) with rainfall intensity over WG (70°-78°E & 8°-21°N) during south west monsoon season, below mentioned methods have been attempted.

i) Inter annual, monthly and daily rainfall variation over WG with respect to AS SST, WS variations.
ii) Monthly correlation has been computed between rainfall over WG & SST over AS for same month and the SST of previous month. To analyse monthly correlation daily SST and rainfall data sets have been utilized.
iii) SST and WS gradient calculation between Somalia coast (7°-12°N, 51°-56°E) and west coast (11°-16°N, 69°-74°E) of India to relate them with monthly rainfall intensity variations over WG. This method has been introduced by Izumo et al. (2008).
iv) SST index and WS index over AS has been estimated to find out in-out phase relationship with rain index over WG. SST index and rain index averaged over AS are estimated as follows

$$SST\ index = \frac{(observed\ \ SST - mean\ \ SST)}{SD} \quad (4.1)$$

$$WS\ index = \frac{(observed\ \ WS - mean\ \ WS)}{SD} \quad (4.2)$$

Any concrete relationship of rainfall intensity over WG with AS SST and WS could not be established following the methods mentioned at (i), (ii), (iii), (iv) (figures are not included). Further to this, the impact of global forced (large scale forcing) for example ENSO and IOD events have been assessed on the following section. NINO 3.4 index and DMI are defined in section 3.2.7 & 3.2.8. Nino 3.4 and IOD monthly indices have been procured and averaged over JJAS months for 15 years (1998-2012). Rain index is calculated over region (8°-21°N & 70°-78°E) as follows

$$\text{Rain index} = \frac{(observed\ \ rainfall\ - mean\ \ rainfall\ )}{SD} \quad (4.3)$$

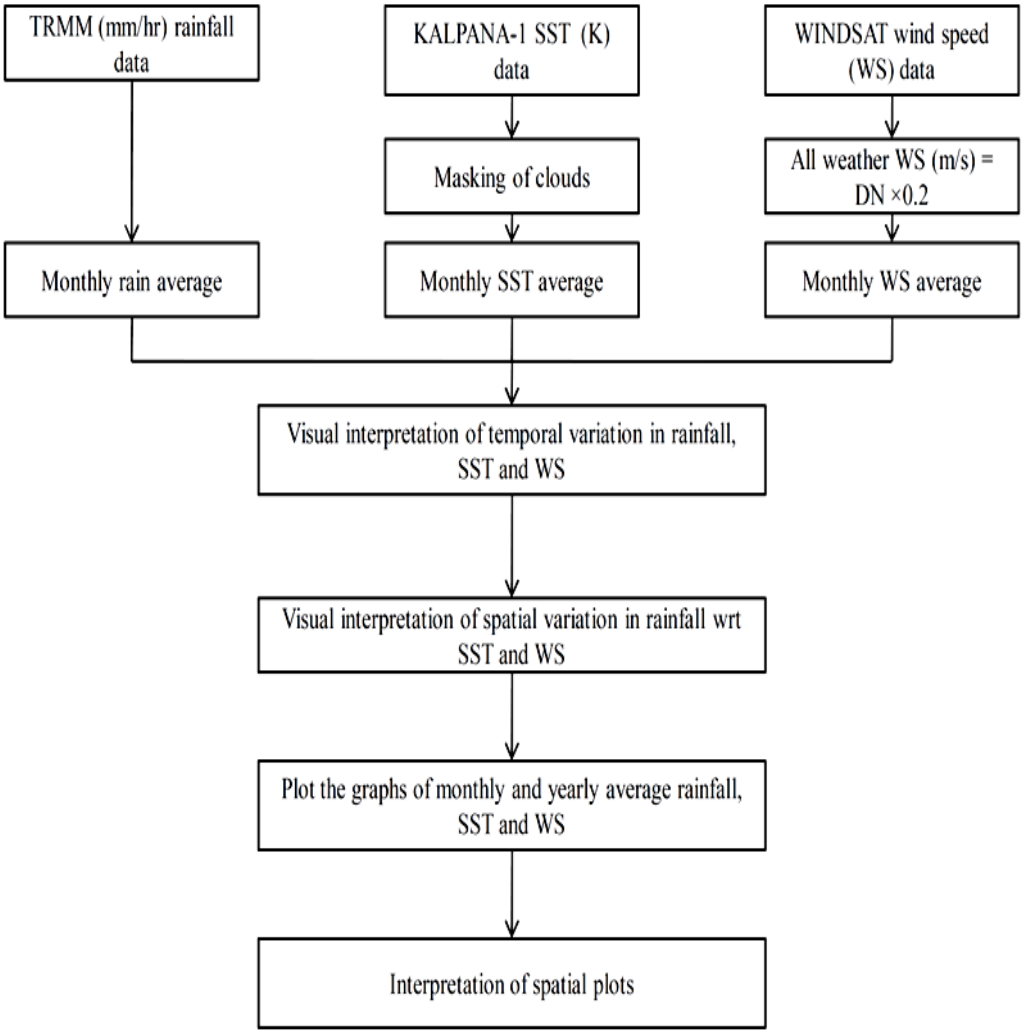

Figure 4.4 Flowchart to observe inter annual and monthly variation in SST, WS and rainfall over WG.

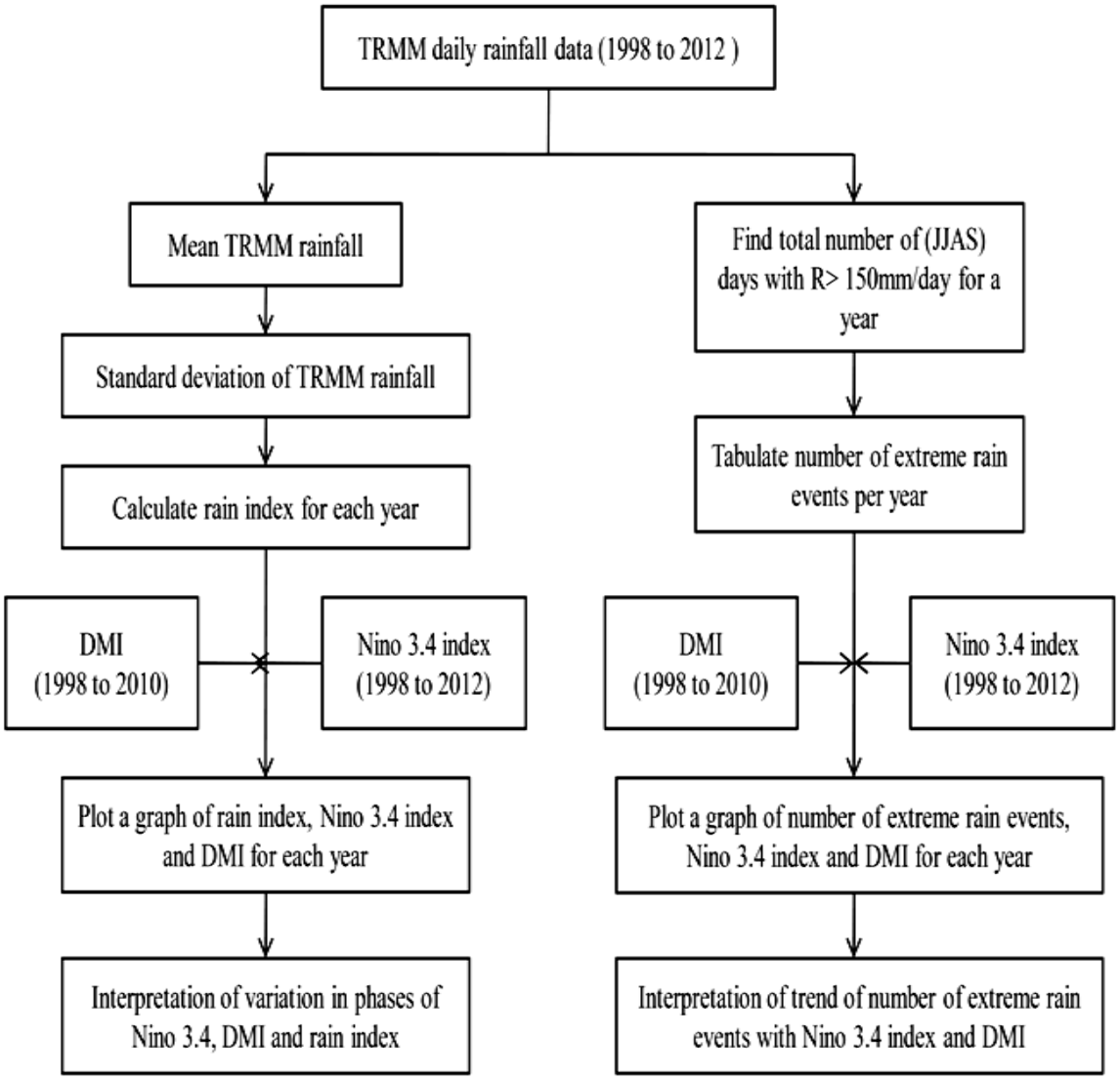

Figure 4.5 Flowchart to observe inter annual variation of Nino 3.4 index, DMI, rain index and number of extreme rain events over WG

4.2.2 Extreme rain events

Extreme rain events in summer monsoon season are selected from the years 2008 to 2012. The intense rainfall events in JJAS months over WG have been picked up. The dates of extreme events have been chosen on the basis of TRMM 3B42 v7 daily rainfall data (mm/day) which considerably matches with that of IMD records in intensity as well as location (pls. refer table 4.1).

Table 4.1 Extreme rainfall events in JJAS months from year 2008 to 2012

No.	Date	Location	Rain (mm/day) from IMD data	Rain (mm/day) from TRMM 3B42 v7
1	28th July 2008	Maharashtra	370	221.5
2	11th Aug. 2008	Maharashtra, Karnataka	490	387.7
3	10th July 2009	Maharashtra	410	333.3
4	31st Aug 2010	Maharashtra	480	247.7
5	16th July 2011	Maharashtra, Karnataka	340	361.4
6	15th June 2012	Karnataka	(Not available)	474.8

The SST, WS and rainfall daily data has been collected for prior and after 5 days of an extreme rain event. The days has been enumerated as (-5 to -1) 5 days prior the event, (0th day) day of event, (+1 to +5) 5 days after the event. The SST and WS data are collected over AS (58°-70°E, 0°-20°N). These three parameters are then scaled up to 0.25° resolution. Before calculating correlation coefficient and significance of correlation, land region is masked in rainfall data, as SST and WS are available only over ocean surface. The flowchart to analyse WS and SST data along with the rainfall variability is given in fig.4.6. Correlation coefficients between SST-rain and WS-rain per day are calculated using formula:

$$\textit{Correlation coeff. (r)} = \frac{\sum(x-\overline{x})(y-\overline{y})}{\sqrt{(x-\overline{x})^2(y-\overline{y})^2}} \qquad (4.4)$$

Where x, y are two variables and $\overline{x}$, $\overline{y}$ are their respective means. Summation is taken over all the data points.

All significance of correlations has been tested at 5% significance level. The formula for estimating the significance is

$$\text{p-value} = r\sqrt{\frac{(N-2)}{(1-r^2)}} \qquad (4.5)$$

Where N is number of data points.

p-value < 0.05 ⟶ Correlation between two variables is significant at 5%
p-value > 0.05 ⟶ Correlation between two variables is significant at more than 5%

Also the spatial scale of significant correlation between SST-rain and WS-rain has been analysed. In this method correlation is not spatially averaged, unlike previous method. Cross-correlation is calculated separately for each location over AS (58°-75°E & 0°-20°N) for 20 days centred on an extreme rain event. The lagged correlations for prior and after 5 days have been estimated. For this cross-correlation calculations SST and WS have been kept as leading parameter and rainfall as lagging parameter.

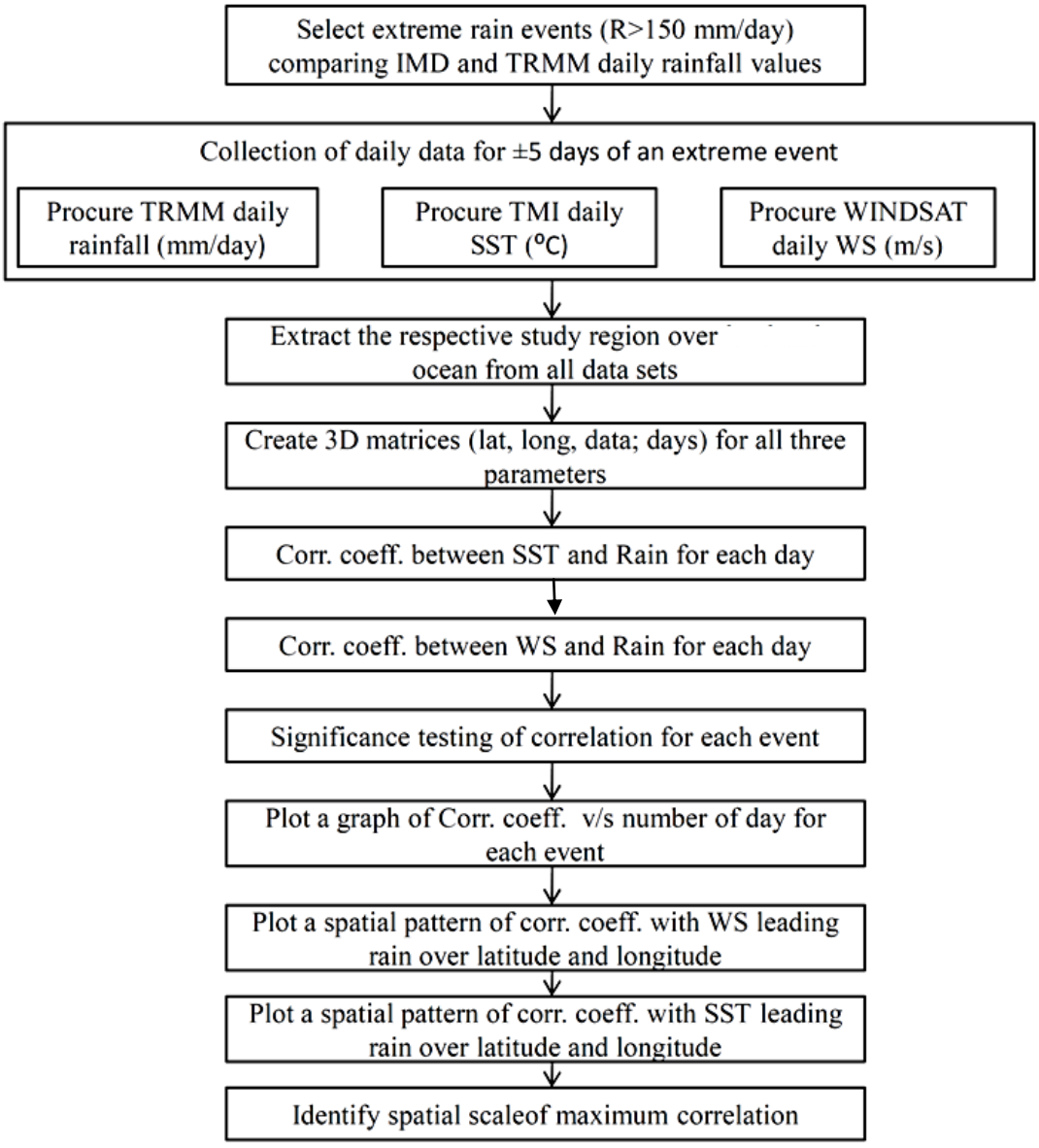

Figure 4.6 Flowchart for lead lag relationship of SST & WS with extreme rain events.

Chapter 5. Results and discussion

5.1 Orographic precipitation over WG

5.1.1 Rainfall

Spatial distribution of long term (14 years) JJAS mean monsoon rainfall from TRMM 3B42 v7 over WG unfolds interesting results as shown in fig.5.1.The mean monsoon rainfall is maximum (about 30 mm/day) over coastal Karnataka followed by Maharashtra (about 20 mm/day) and Kerala (about 14 mm/day). Intensified rainfall appears near west coast and its adjacent oceanic region and the rain shadow region (R<6 mm/day) to the East of WG barrier. In the present study rain shadow region is considered as a region where seasonal mean rainfall drops down to 1/5th of maximum rainfall (30mm/day) observed over study region. Maharashtra and Kerala has 50-100 km belts of homogenous rainfall intensity in latitudinal direction, while in Karnataka, rainfall regimes varies at every 25km. Fig. 5.1 displays high rainfall is distributed approximately up to 75km from Karnataka coast line. After that rain shadow region starts at 75°E (at 15°N) and 76°E (at 12°N) with eastward dispersion of 100-250 km. In Maharashtra rain shadow area expands after 74°E. Rainfall intensity gradually steps down from North to South in Kerala which is consistent with earlier studies (Soman et al.1988; Simon & Mohankumar,2004; Krishnakumar et al.,2009).

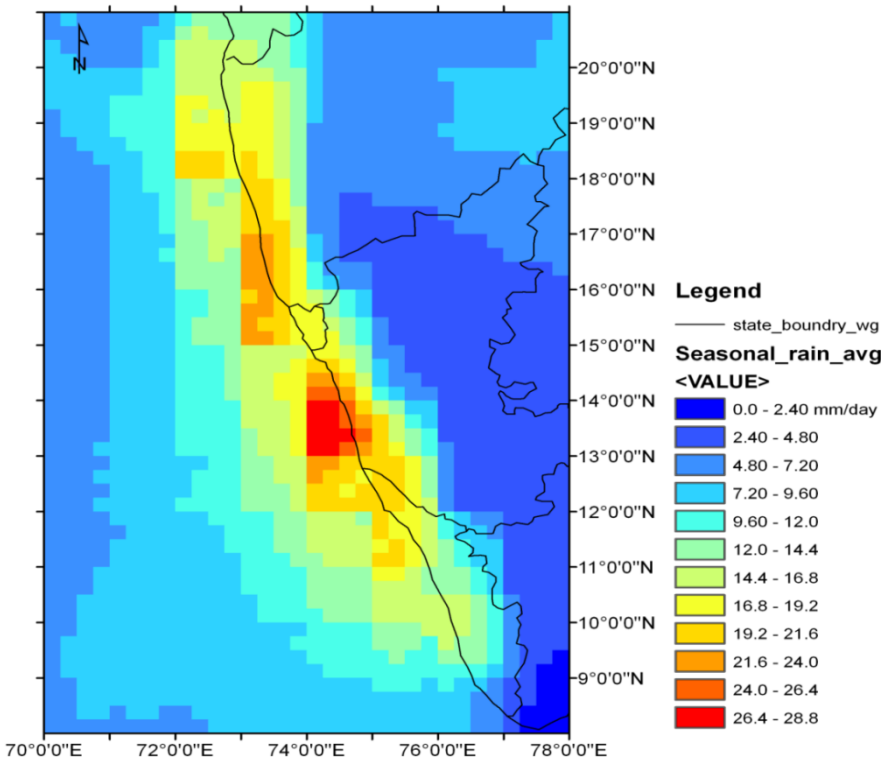

Figure 5.1 Spatial pattern of rainfall in summer monsoon season (JJAS) unravelled by TRMM 3B42 v7 satellite estimates at finer spatial resolution (0.25°) over WG. The rainfall is averaged over 14 years (1998 to 2011). Colour bar indicates intensity of rainfall in mm/day.

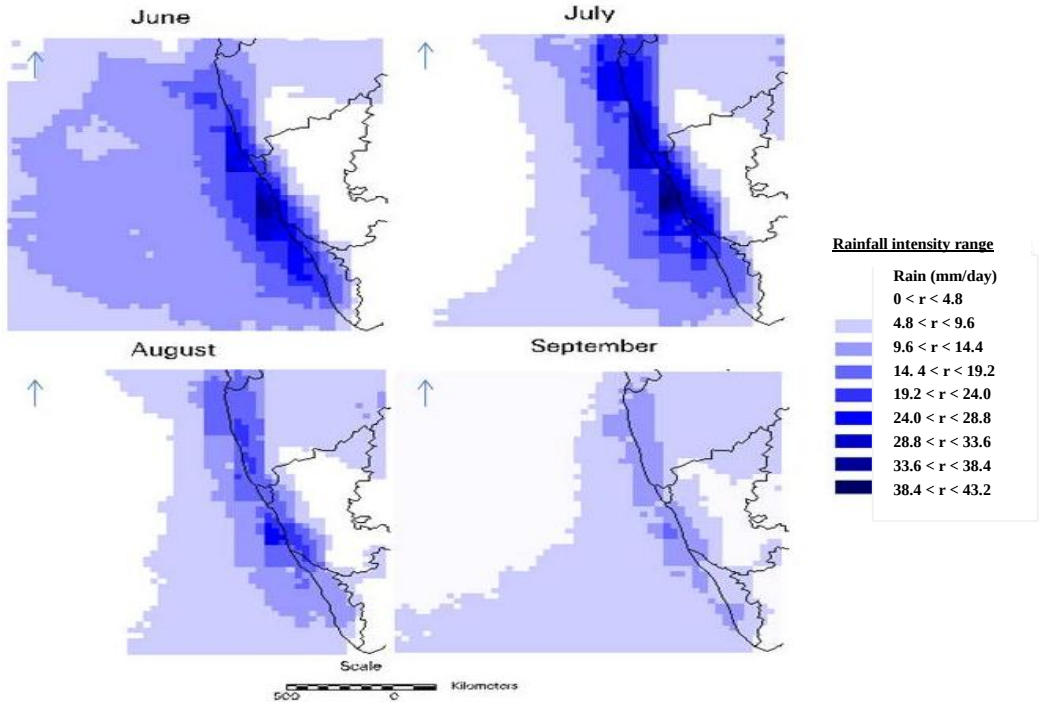

Figure 5.2 Spatial distribution of monthly rainfall during south west monsoon season over WG (65°-78°E, 8°-21°N). Rainfall is averaged over 14 years (1998-2011). Colour bar indicates rainfall intensity (mm/hr). Figure is prepared in ERDAS Imagine software.

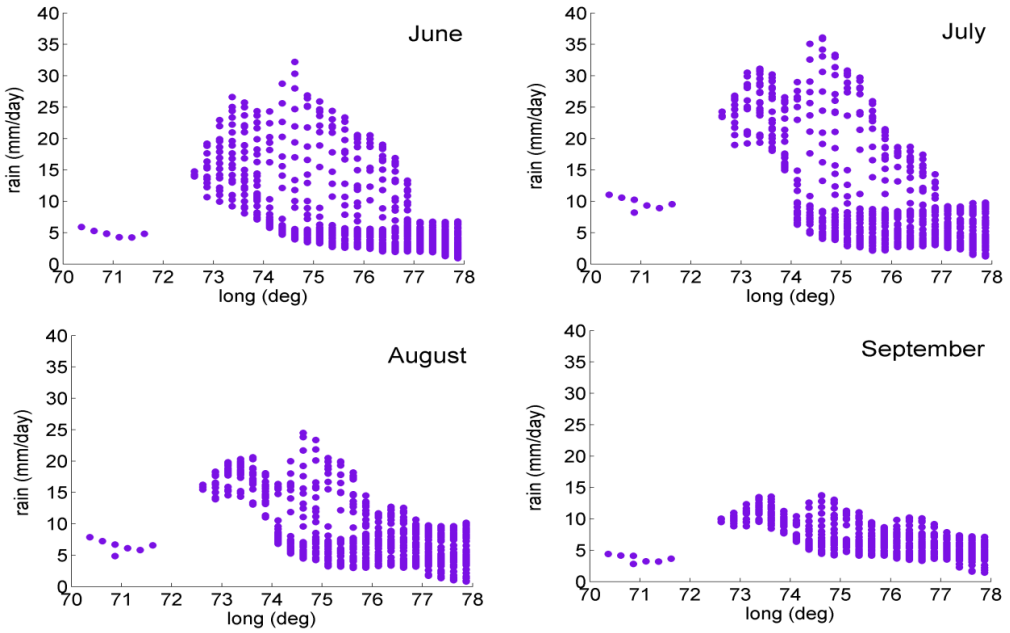

Figure 5.3 JJAS rainfall distribution in longitudinal cross section over WG. Rainfall is averaged over 14 years (1998-2011).

In addition to spatial variability in rainfall patterns over WG, the temporal variability in orographic rainfall has also been analysed. Fig. 5.2 shows monthly rainfall time series over study region. In June and July, the rainfall intensity along the west coast of India is found to be maximum. During August-September, rainfall activity reduces over study region. The spatial distribution of orographic rainfall along the WG is found to be same in all the months of south west monsoon season. The longitudinal extent of rainfall in JJAS months is plotted in fig. 5.3. It also reflects that the rainfall follows similar spatial pattern in JJAS except heavy rainfall events are more in June-July whereas moderate and low rainfall events are more in August-September.

5.1.2 Spatial variation in topography of WG:

Analysis of ASTER DEM data (please refer to fig. 5.4) reveals that Maharashtra has cascaded, narrow and linear mountain belt whereas Kerala has isolated, narrow mountain range. Cascaded and broad mountain barrier is identified at Karnataka. The spatial variability of rainfall has been studied with respect to the variation in topographic front of WG. Present analysis reveals that heavy precipitation is found in Karnataka followed by Maharashtra and then Kerala. It ascertains that cascaded mountains induce intense rainfall compared to isolated mountains. One possible reason behind this could be the spatial extend of horizontal flow restricted by the isolated mountain is less compared to the chain of mountains. It has governed in the study of Kirshbaum & Smith (2008) that advection time scale determines amount of precipitation. Advection time scale (Ta) is a ratio of horizontal width of mountain by incident horizontal flow velocity i.e. Ta is proportional to width of barrier if horizontal wind speed is kept constant. Broader mountain contributes to longer Ta which further provides sufficient time for condensation of uplifted moist flow to grow and precipitate before evaporating to leeward side of barrier. This concept is also explained by Jiang & Smith (2003), Elliott & Hovind (1964). It suggests that broader mountains of Karnataka receive more precipitation as compared to narrower mountain barrier of Maharashtra. Conversely broader mountain barrier strengthens rain shadow region on the leeward side. Consequently, the leeward side of Karnataka receives very less rainfall (<4mm/day) as compared to lee ward side of Maharashtra (<6mm/day). Also it has been observed that rainfall reaches its maximum on the upwind side before summit has encountered and reduces in sharp amount after that i.e. maximum rainfall doesn't occur on the line of highest altitude, this fact is also reported by Mukherji et al. (1972). This may be because of falling particles get enough depth to grow by collision and coalescence at the foot of the mountain compared to the top of the mountain (Elliott & Shaffer, 1962).

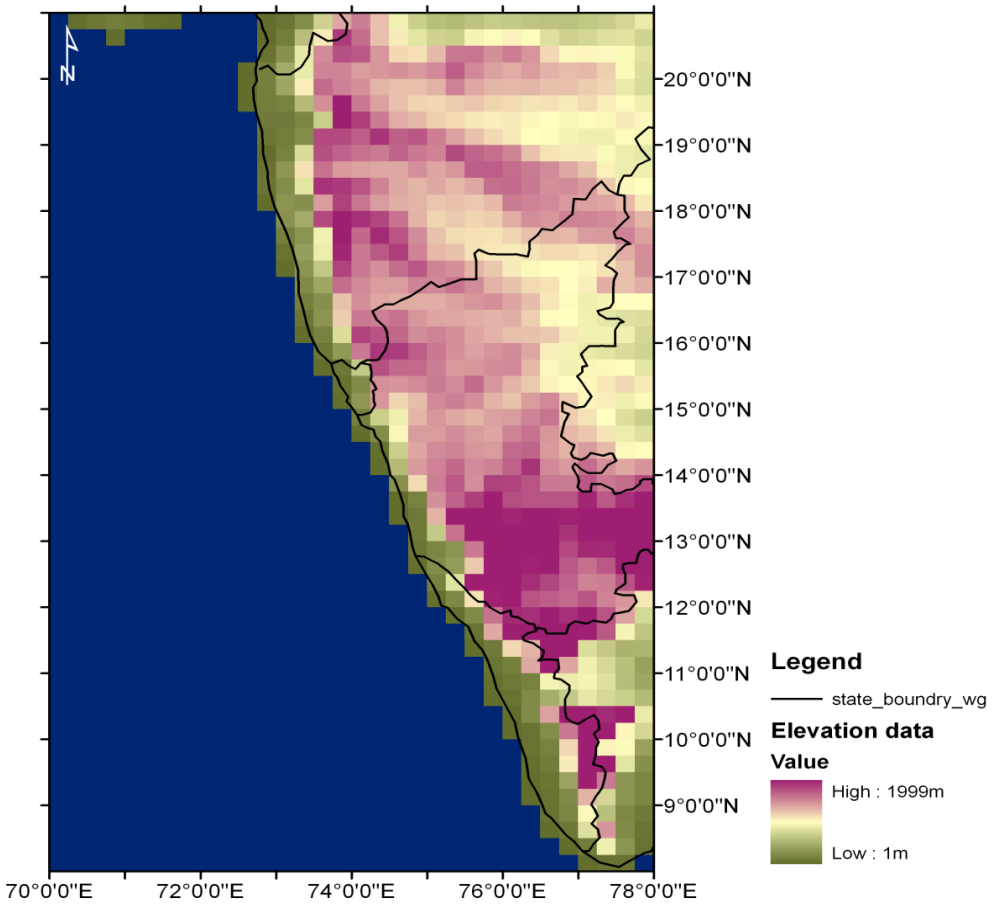

Figure 5.4 ASTER GDEM data resampled from 30m to 25 km over WG (in image processing software ENVI). Colour bar indicates elevation in meters.

5.1.3 The WG elevation:

Fig. 5.5 displays variability in elevation over study area. Two eminent and isolated peaks are observed in Kerala. The sudden deep in elevation (less than 400 m) between these two elevated mountains is known as 'Palghat gap'. The mountain crests are found to be higher in Karnataka than in Maharashtra. Also the extent of high elevation is discovered to be well spread in Karnataka. The analysis of variability in elevation in the context of spatial distribution of rainfall infers that, increment in elevation intensifies rainfall and rainfall declines before it confront summit of barrier. This observation is in accordance with the result given by *Das* (1968), that monsoon air begins to rise at about 50km before the crest of mountain in WG. At Palghat gap and low elevation locations of WG barrier (i.e. Karnataka at 14.50°-15°N elevation ranges between 500 to 600 m) rainfall is less compared to its surrounding mountains having height more than 600m which concurs with observations of Raj & Azeez (2010). Present analysis suggests that the specific control exerted by the elevation of the mountain barrier in WG is limited to certain height. Statistical data listed in the table 5.1 determine that

the elevation around 800m in WG acts as hermetic to incoming wind. It suggests that there could be atmospheric blocking at around 800m either due to weak wind speed or presence of temperature inversion layer (i.e. stratification layer). This observation needs further investigation. After analysing longitudinal extent of some of the spatial locations which receive highest rainfall in WG, a paradox is observed to the direct proportionality of elevation and precipitation. It is illustrated in the fig. 5.6 that for a particular case higher mountain may receive less precipitation than mountain with shorter height. For an example, in Maharashtra, mountain of height 638m receives more rainfall than mountain with height 712m. It has also been observed that some of the mountains of WG give inverse relation between height and precipitation. Therefore in order to quantify more precise relationships between orography and rainfall we studied the rate of change of elevation at every 25km.

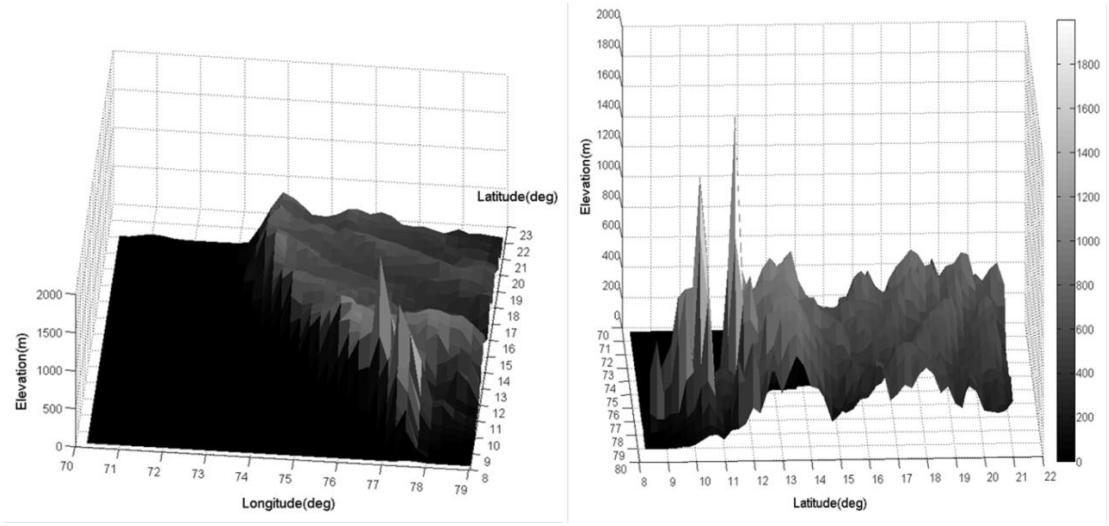

Figure 5.5 ASTER elevation data at 25 km resolution represented at two different view angles. It depicts variation in elevation and topography of WG i.e. Kerala state has two highest but isolated apexes. Colour bar indicates elevation in meters.

Table 5.1 Long term monthly rainfall peaks observed over WG barrier and its corresponding elevation.

Month	Longitude (deg)	Rain(mm/day)	Height(m)
June	74.50	32.217	770
	74.25	28.7616	773
	73.50	25.7232	770
	74.75	26.8848	701
	77.00	6.4	1645
July	74.25	35.0904	770

	74.50	36.108	753
	74.75	33.3576	701
	77.00	9.18	1645
August	74.50	24.4752	753
	74.75	23.3592	701
	73.50	20.472	770
	75.00	20.4792	639
	77.00	9.74	1645
September	74.50	13.776	753
	74.75	13.0272	701
	73.50	13.5432	770
	77.00	9.17	1645

5.1.4 Spatial variability of elevation in WG:

Slope information of the mountainous terrain provides the spatial variability in elevation at defined unit distance. The slope considers maximum change in elevation between one granule and its neighbouring granules. The analysis of spatial distribution of slope contradicts the information given by Tewari (1995) about steepness of WG barrier. The results based on the ASTER GDEM data sets and slope distribution of WG reveal that the slope of the mountains in Karnataka are gradually increasing as compared to the slope of WG barrier in Maharashtra and Kerala. Slope and rainfall extent in longitudinal direction of WG (fig.5.8), portrays two peaks; one with abrupt raised slope and other with gradually increasing slope. Spatial distribution of slope and rainfall of WG brings out that the rainfall amount slews in direct proportional to the degree of slope. As reflected in fig. 5.8 slopes with gradual change are prone to induce more precipitation than slopes rising abruptly. As mentioned in previous section, in Maharashtra, mountain of height 638m induces more rainfall than mountain with height 712m. Same points have been observed (fig. 5.7) with slope data i.e. at 16.50N and 15.75N in Maharashtra state. Fig. 5.7 also depicts that rainfall pattern mimics the slope line of mountain front. It also reveals that mountain with higher elevation and abrupt changing slope leads to less precipitation at the foot of that mountain compared to mountain with lesser height and gradual changing slope. One possible mechanism behind this could be inferred as that gradually increasing slopes provide stable ascent to incoming air parcel which would deflect upward after striking WG barrier (Sarker, 1966; Grossman & Durran, 1984; Ogura & Yoshizaki, 1988). In this situation the air parcel has to spend less energy against gravitational pull hence would retain its velocity for longer time. This would also provide sufficient vertical motion of cloud droplet to grow by collision and form precipitation, as concluded by Sumner

(1988). The gradually increasing slope is also capable of providing large surface area to incoming solar radiation and hence raising the convective activity. This fact has also been mentioned by De & Dutta (2005) that mountains slope acts as source of heat to produce convection cells and the air parcels then converges at the top of the mountain.

We have also analysed aspect map of WG and observed that almost all the mountains in WG region are south-west facing (figure in not shown).

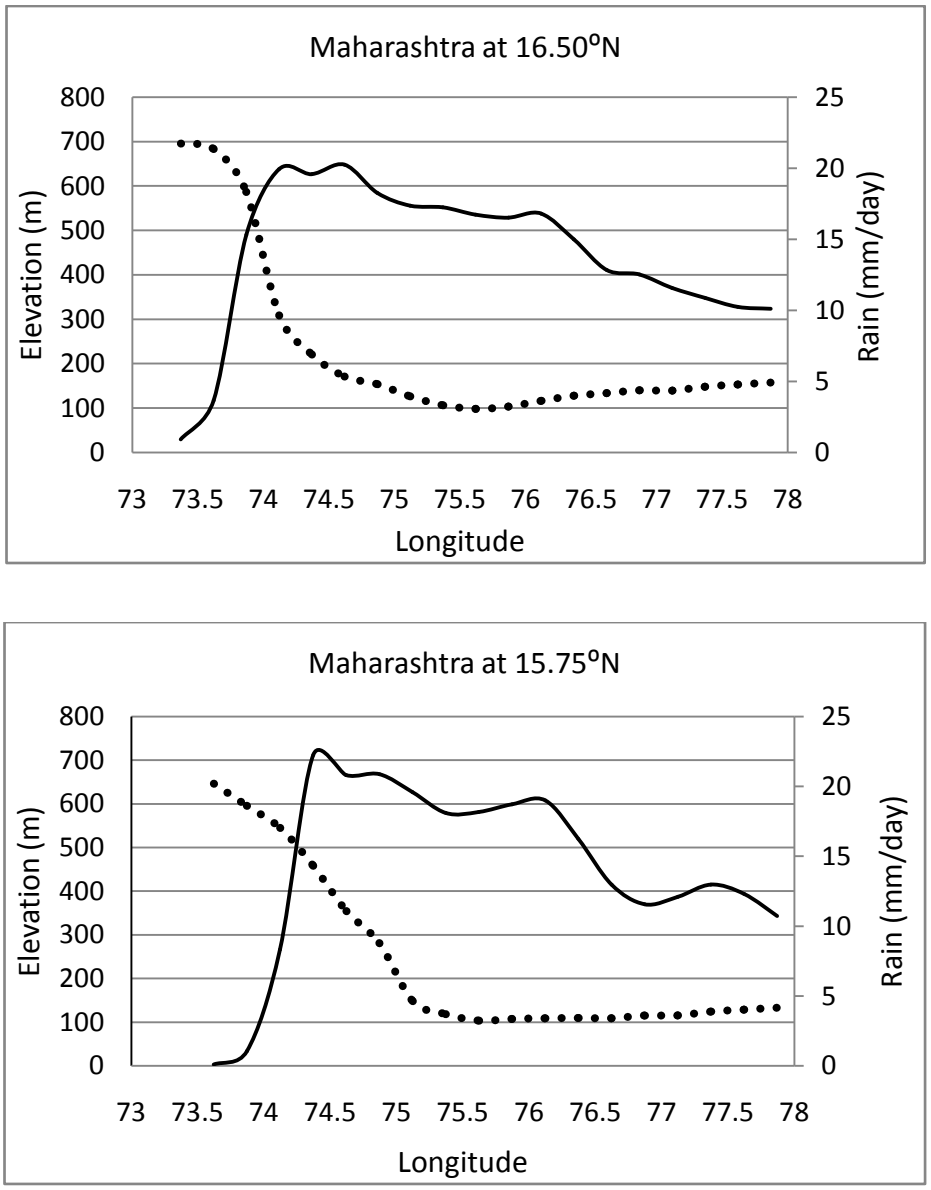

Figure 5.6 Longitudinal extent of elevation and corresponding rainfall profile at 16.50N and 15.75N. (—) is for elevation in meters. (•••) is for rain (mm/day). Elevation and rain is plotted on Y axis. Longitudes in degrees are on X axis.

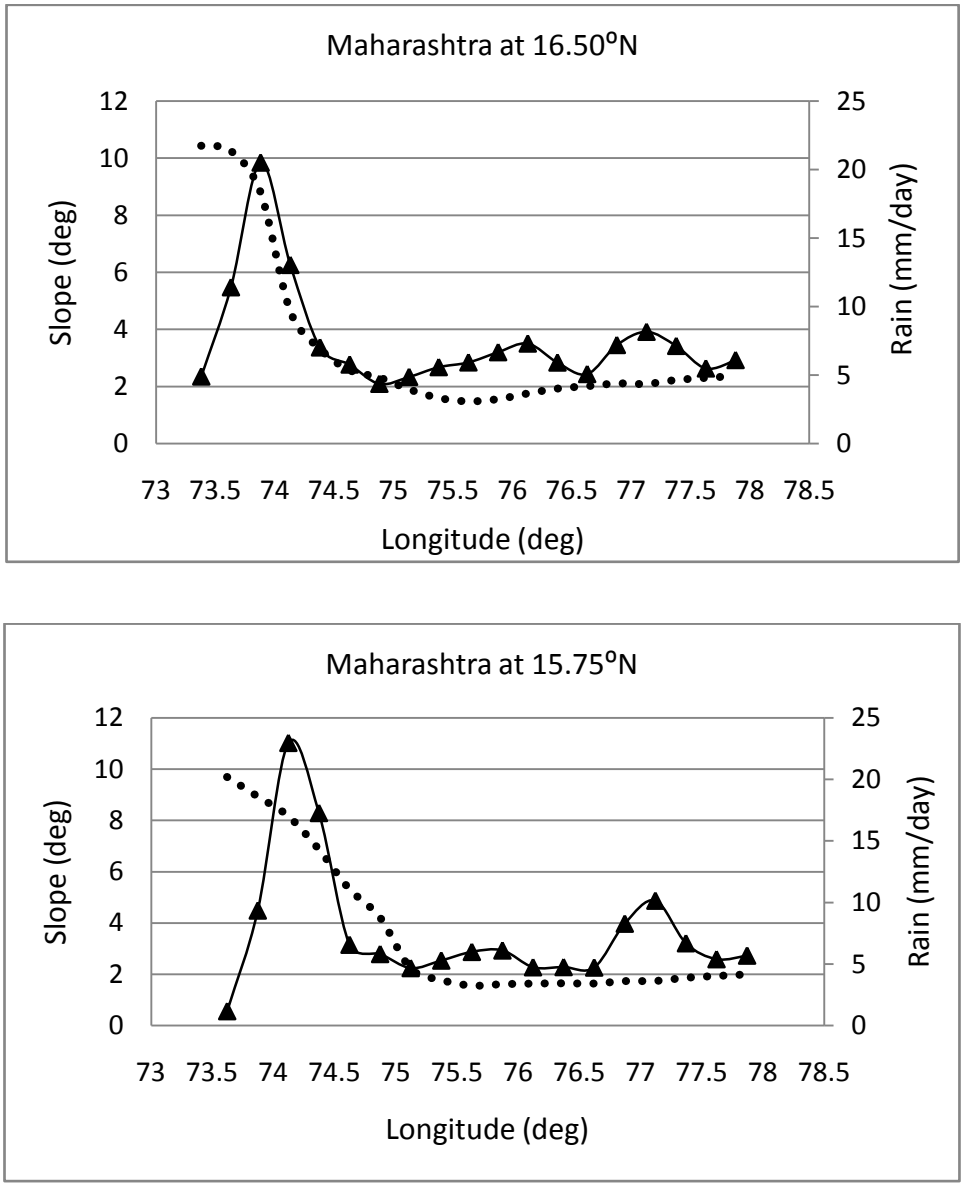

Figure 5.7 Longitudinal extent of slope and corresponding rainfall profile at 16.50N and 15.75N. (▲—) is for slope in degrees. (•••) is for rain (mm/day). Slope and rain is plotted on Y axis. Longitudes in degrees are on X axis.

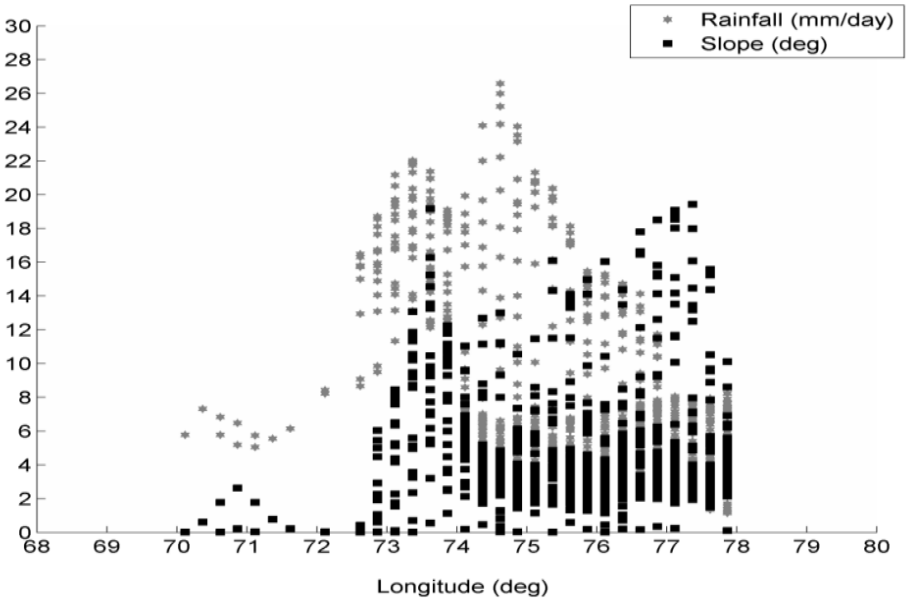

Figure 5.8 Longitudinal extend of slope and rainfall is plotted. Y axis represents slope (deg) and rainfall (mm/day) distribution considering only land region. It is clearly seen that the WG's slope has two prominent peaks, first with abrupt change in slope and second peak with gradual increasing slope. Rainfall over gradually increasing slope is high.

5.1.5 Extreme rain events in WG:

A spatial plot in fig. 5.9 represents the total number of extreme rain events occurred at every grid in last 14 years over WG and its adjacent oceanic region. For this purpose two thresholds are set as documented in methodology section; (150 mm/day >R > 120mm/day) and (R> 150 mm/day). Heavy rain bouts are least observed in Kerala state. The results show that the prone area of extreme rainfall events for the threshold of (150>R>120 mm/day) is between 16.25°-17.25°N & 73.25°-73.75°E in Maharashtra with approximately 2 events per year. In Maharashtra, the area between 16.25°-16.50°N & 73.25°-73.50°E receives approximately 3 extreme events (R>150 mm/day) per year. The second place captured is near Mumbai in Maharashtra between 18° to 19°N (approx. 2 events per year). Similarly, the prone area of extreme rainfall events for threshold of (150>R>120 mm/day) is between 13.50°-14.50°N & 74.50°-74.75°E in Karnataka. This location receives approximately 2 extreme rain events per year. At Karnataka, it is found that the location 13.75° to 14.50°N also encounters approximately 2 extreme rain events per year for the threshold of R>150mm/day. These locations are in context with results documented by Francis & Gadgil (2005). It has been observed from spatial distribution of number of heavy rain events that the mean monsoon rainfall received by windward side of Karnataka is highest during south west monsoon but extreme rainfall events (R>150 mm/day) are more frequent near coastal Maharashtra. A case study is carried out in association with above spatial distribution of heavy rain events which reveals that the extreme downpour on 17th June 2012 at Ratnagiri (Maharashtra) occurred

between 16° to17°N, near Konkan railway stations (16.50° to17°N). This location is detected by TRMM 3B42 v7 daily rainfall estimations as a location of frequent extreme rain event in WG (please refer fig. 5.9) during last 14 years period (1998 to 2011). All these locations have also been examined in association with topography and elevation which could not provide any profound information, however slight dips in elevation have been observed which may lead to valley effect and intensify rainfall at respective locations.

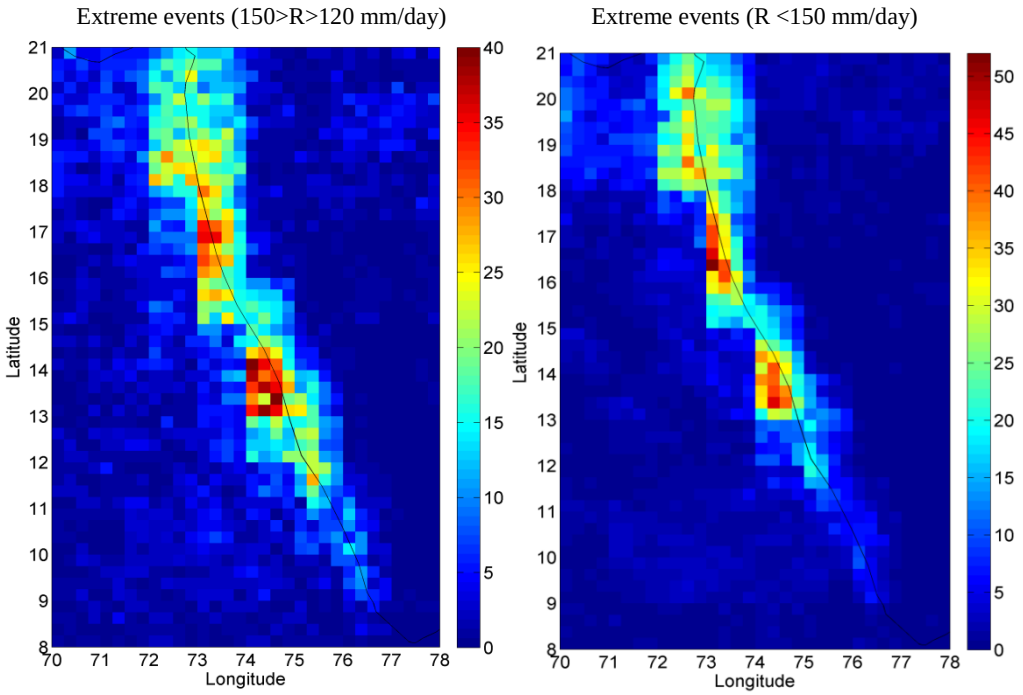

Figure 5.9 Spatial distribution of heavy rainfall (150>R>120mm/day & R>150mm/day) events over WG. Colour bar indicates number of events occurred in last 14 years. Red colour depicts highest number while blue indicates lowest number of heavy rain events.

5.2 SST, WS, OLR variations with WG's rainfall:

5.1.1 Inter annual variability of rainfall over WG:

It has been discussed in the data analysis section that KALPANA-1 SST data is reliable from year 2010 onward for JJAS months. Therefore only three years of KALPANA-1 SST data have been utilized to study the monthly variations in AS SST as well as WS during south west monsoon over WG. Fig. 5.11 depicts variations in SST of AS and Indian Ocean in JJAS months. Blue colour is representative of colder SST while pink colour is of warmer SST. It has been observed that in June, upwelling initializes at Somalia coast and SST gradient develops between eastern and western AS. The incoming south westerly winds from equator causes upwelling along Somalia coast which shifts warm surface water towards west coast of India. During developing phase of monsoon in July, upwelling at Somalia continues to propagate colder water towards west coast of India. The cooler SST anomaly raises the sea level pressure

over AS and hence diminishes the evaporation (Shukla, 1975). In August, eastward advection of colder water in AS is highest (pls. refer fig. 5.11). And also high rainfall in June-July, water run-off from land and intense cloud cover near west coast of India attribute to the significant decrease in SST over entire AS. From June to August cooling phase of AS SST has been observed. In September, SST in AS again starts rising due to the weakening in differential heating between land and ocean. This suggests that AS state modulates the ISMR but by referring fig. 5.10 it has been observed that there is no strong interdependence of AS SST on the intensity of ISMR.

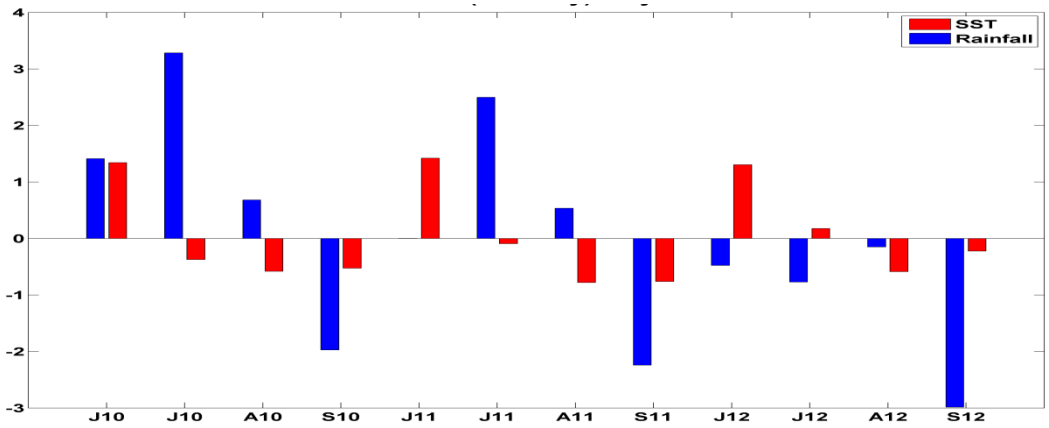

Figure 5.10 SST and rain indices in JJAS months from year 2010 to 2012. X axis represents JJAS months per year. Y axes represents magnitude of indices. Red bar chart indicates SST departure form mean SST in AS. Blue bar chart indicates departure of rainfall over WG.

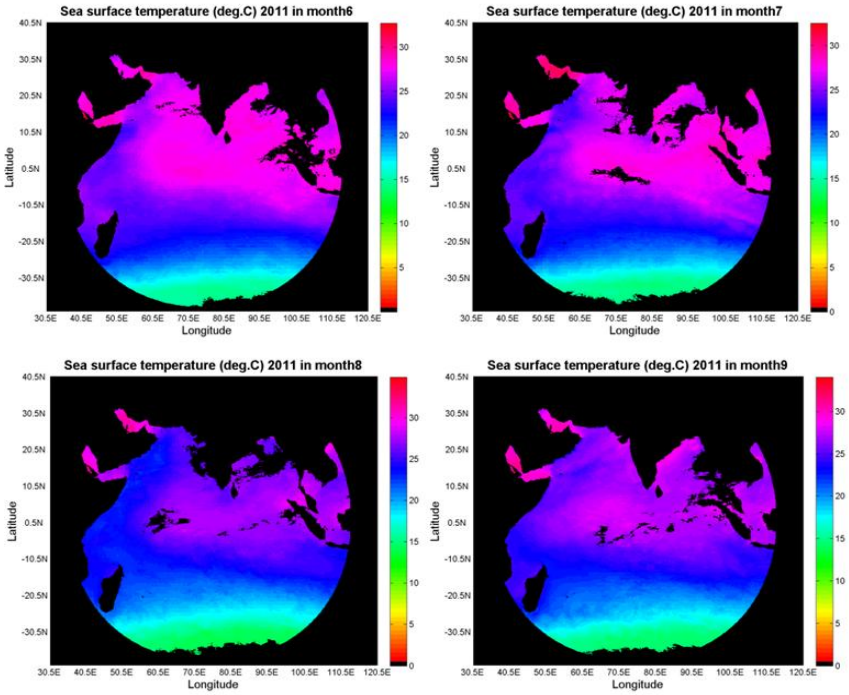

Figure 5.11 Monthly SST (°C) variations in Arabian and Indian Ocean in summer monsoon season (year 2011). Pink colour indicates highest SST while green colour indicates lowest SST.

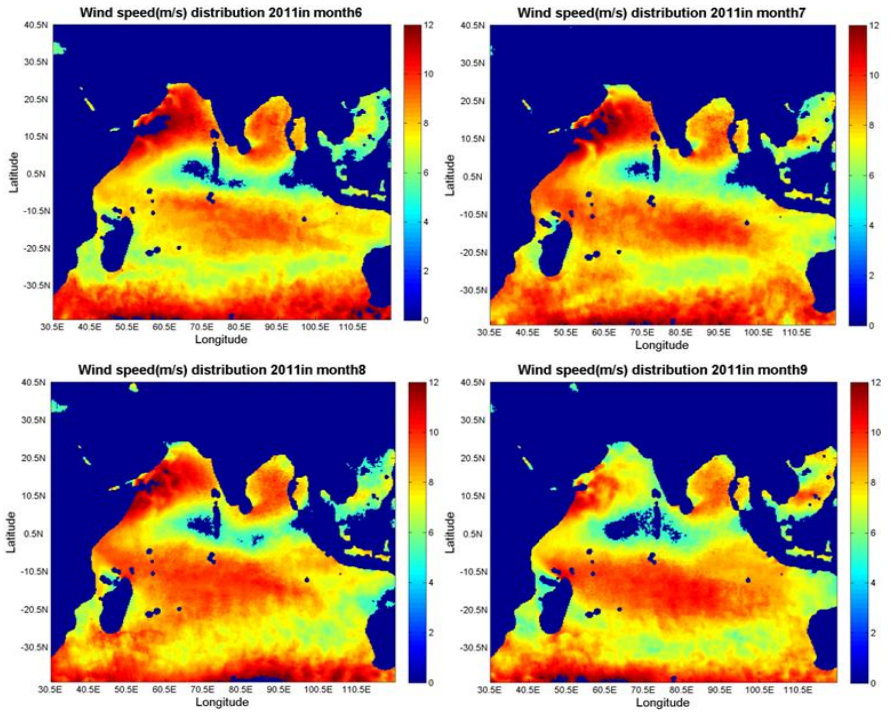

Figure 5.12 Monthly WS (m/s) variations in Arabian and Indian Ocean in summer monsoon season (year 2011). Red colour indicates highest WS while blue colour indicates lowest WS.

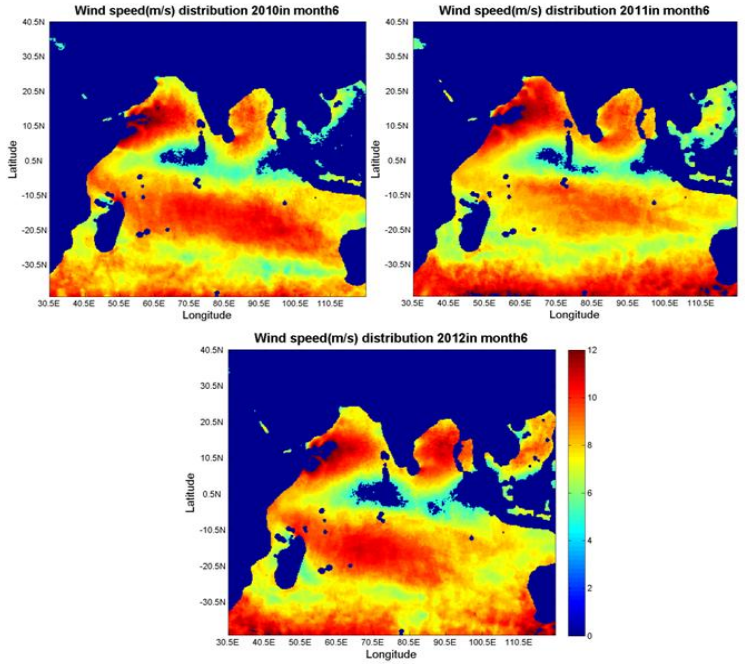

Figure 5.13 WS (m/s) distribution over Arabian and Indian Ocean for three different years during south west monsoon (June month). Red colour indicates highest WS while blue colour indicates lowest WS.

Spatial distribution of wind speed for JJAS months is shown in fig. 5.12. It depicts that wind speed peaks (up to 12 m/s) during early summer monsoon season i.e. in June and July near Somalia coast and starts decreasing from August-September. Wind direction in summer monsoon season is from Somalia coast to West coast of India (i.e. westerly) and extends up to BOB (Bay of Bengal) and hence moisture transport is from Somalia coast to BOB (figures are not included). In south west monsoon season a strong pressure gradient develops between land and ocean surfaces in June and July. This introduces increment in WS and hence along shore upwelling at Somalia coast. It has been observed that weaker than normal south westerly winds in late monsoon over western AS again increases SST (refer fig 5.11 & 5.12 for September) of AS. The analysis of yearly accumulated rainfall of JJAS over WG (65-78E, 8-21N) reveals that WG received maximum rainfall in year 2010. Rainfall intensity is found to be maximum in all JJAS months in 2010 followed by in a year 2011 and then in year 2012. The WS pattern shown in fig. 5.13 suggests that winds travelling from AS to the BOB are stronger in year 2012. Weak WS at BOB in year 2010 provides sufficient residing time for moisture to condense and precipitate over AS in respective year. All above results suggests that along shore variability of WS strengthens/ weakens the upwelling at Somalia coast which affects the source of moisture (i.e. extent of warm pool) in AS and departs the rainfall over WG.

As it has mentioned earlier, the analysis of behaviour of SST and rainfall considering their departure from normal (considering fig. 5.10 and also the methods explained in methodology section 4.2.1) in JJAS reveals that AS colder anomaly affects the rainfall over WG but it is not the only factor that controls the rainfall intensity over WG .This result is in concurrence with the results of Shukla (1975) considering AS SST and ISMR. To understand the effect of global circulation on rainfall over WG, the annual rainfall departures have been studied in response to ENSO cycles and IOD events. It has been observed that the effect of ENSO coupled with Indian Ocean dipole can effectively explain inter annual rainfall variations as compared to the association of Arabian SST variations with rainfall. Fig 5.14 displays the departure of NINO 3.4 and DMI indices from year 1998 to 2012 with corresponding rain index over study area. To monitor the departure in ONI values, NASA has defined El Nino and La Nina events as follows, when NINO 3.4 index exceeds the value 0.5 it is consider as El Nino event and when NINO 3.4 index recedes -0.5 it is consider as La Nina event. La Nina is generally associated with strong summer monsoon rain over Indian sub continent (Clark et al., 2000). Similarly positive DMI means below normal or cold SST anomalies over south-eastern Indian ocean (Sabeerali et al.,2012; Saji et al,1999), this event is considered as IOD. A positive DMI indicates higher rainfall over Indian subcontinent (Saji et al ,1999; Rao et al, 2010).

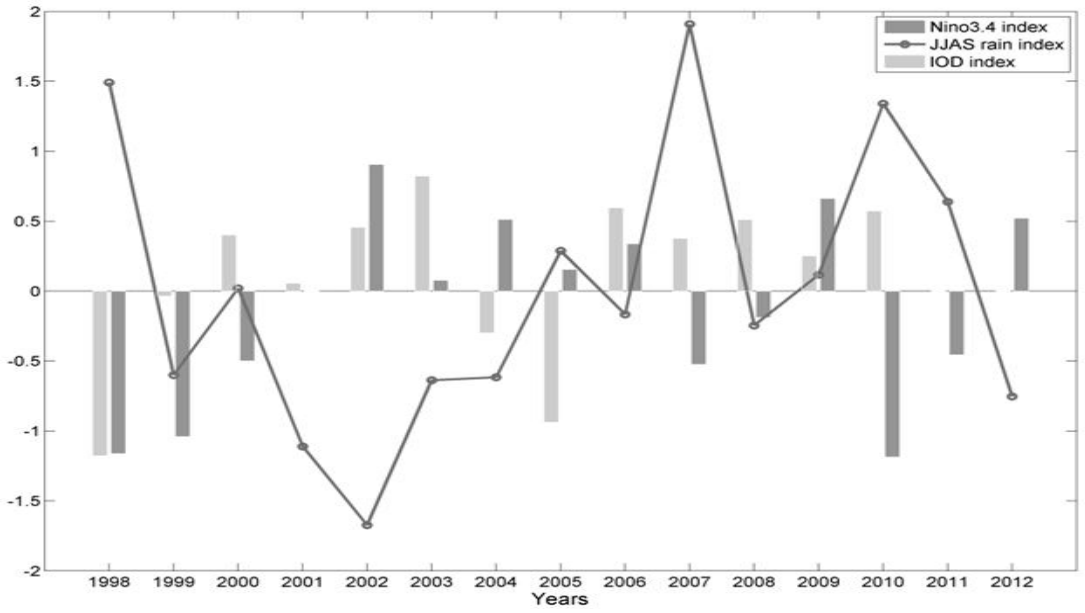

Figure 5.14 NINO 3.4 Index (blue colour bar) & IOD Index (gray colour bar) with rain index (blue line) for last 15 years. X axis is year and Y axis are indices varying from ±2.

From fig. 5.14, it has been observed that NINO 3.4 index less than -0.5 induces above normal rainfall over WG (except in year 1999). This negative NINO 3.4 index referred as La Nina event in equatorial Pacific Ocean is result of below normal averaged SST defined in NINO3.4 region with a warmer western Pacific SST. During La Nina, sea level pressure decreases at western Pacific due to excess evaporation and convection over western Pacific. Consequently wind travels from east to west. These strong easterlies pile up warm water in western Pacific introducing gain in rainfall over Indonesia and Indian subcontinent [http://www.meted.ucar.edu]. Fig. 5.14 also concludes that the deficient rainfall over WG is associated with NINO 3.4 index greater than 0.5 i.e. year 2002. Negative rain anomaly (i.e. below normal rainfall) is associated with positive Nino 3.4 Index except in year 2008, a reason for this exceptional year 2008 is explained by Rao et al. (2010). By analysing the inter-annual variation of IOD with annual rainfall fluctuations and ENSO cycles in JJAS months, we can conclude that IOD events have secondary impact on rainfall regimes over WG. Even in El Nino condition of Pacific Ocean, a positive IOD increases mean south west monsoon rainfall over WG. Ajayamohan & Rao (2008) documented the fact that IOD event is moderately correlated with seasonal mean rainfall over central India. By analysing the departure of rainfall from its mean with ENSO and IOD events it has been concluded that rainfall intensity over WG in south west monsoon season is govern by both ENSO and IOD events but El Nino/ La Nina event seems to suppress the IOD effect over WG's rainfall (Coorelation coeff. of ENSO-rain is -0.2628 (p-value=0.34) and IOD-rain is 0.2247 (p-value=0.46)).

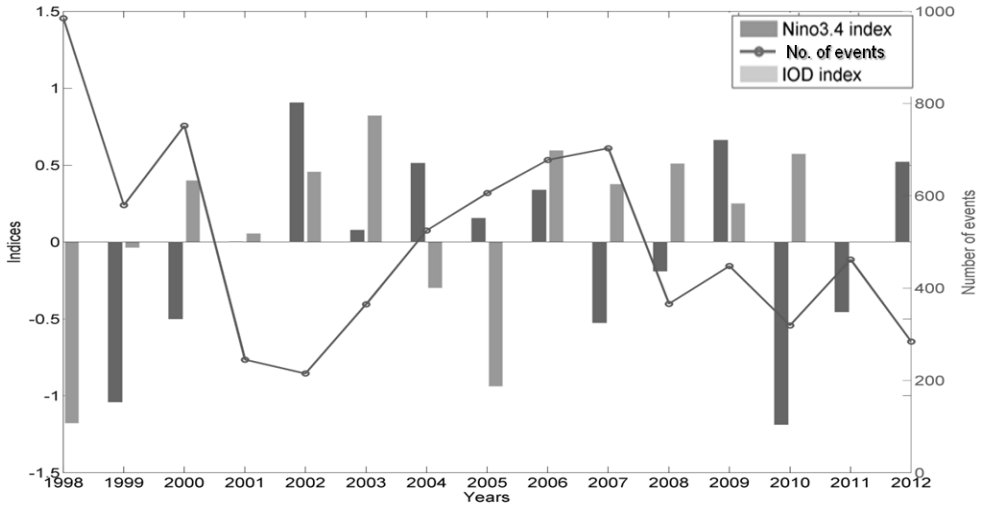

Figure 5.15 Trend of NINO 3.4 Index (blue colour bar) & IOD Index (gray colour bar) with number of extreme rain events (r>150 mm/day) (green line) for last 15 years. X axis is year and Y axis are indices and number of events.

Further to this, the IOD and ENSO impact on number of extreme events over WG in summer monsoon season has been analysed (fig. 5.15) using 15 years TRMM 3B42 v7 rainfall data. The trend of frequency of extreme rain events per year has been studied with respect to DMI and NINO 3.4 indices. The study of Ajayamohan & Rao (2008), concludes that El Nino do not show significant correlation with number of extreme rain events over central India while IOD events are likely to increase number of extreme rain events over central India. By analysis fig. 5.15, we observed that the frequency of extreme rain events over WG are not modulated by IOD as well as ENSO events (correlation coeff. between ENSO-no. of extreme rain events is -0.4642, significant at of 9% significance level & correlation coeff. between IOD-no. of extreme rain events is -0.5394, significant at of 6% significance level).Therefore the developing phase and impact of local circulation has been investigated by observing AS state (SST and WS) condition before an extreme downpour (refer section 4.2.2).

5.2.2 Extreme rain events over WG:

Event1: 28th July 2008

According to IMD monsoon report (2008), an extreme rain event was observed near coastal Maharashtra with rainfall intensity 370mm/day on 28th July 2008. TRMM 3B42 v7 satellite records 221.5mm/day rainfall on the same date at the same location. TRMM 3B42 v7 rainfall records show that rainfall intensity was more than 150mm/day 5 days prior of the event. Referring fig.5.16, it has been observed that from 5 days to 2 days prior of the event, correlation between WS-rain is constant. An increased positive correlation is observed from 1 day prior to 1 day after the event. Correlation between SST-rain shows less fluctuation and decreases to minimum on the day of an event. All correlations are significant at 5% significance level. Correlation has been computed over all locations of AS for 5440 data points.

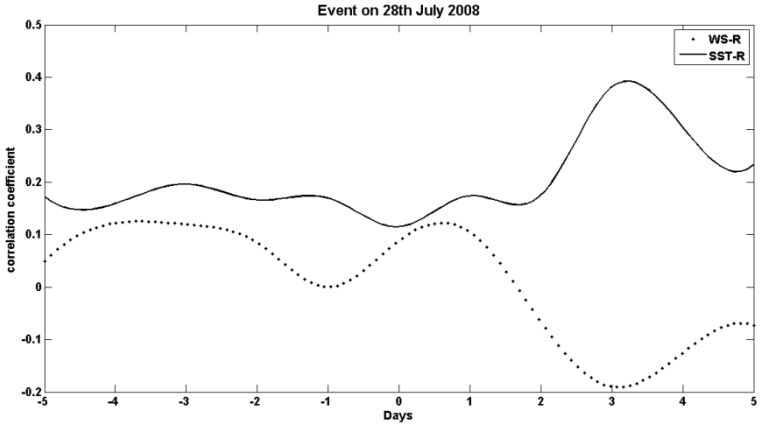

Figure 5.16 Extreme rain event on 28th July 2008. Y axis denotes correlation coefficient and X axis denotes number of days from the day of an event. Dotted line represents correlation between WS and rain while solid line is for SST and rain. 0th day is referred as the day of an event.

Event2: 11th August 2008

The prolonged extreme rainfall event near Maharashtra and Karnataka has occurred from 10th August to 13th August 2008, according to IMD monsoon report (2008). The accumulated rainfall per day was 440, 490, 350, 270mm respectively. Heavy rain is recorded from prior 1 to 2 days after an event. TRMM 3B42 v7 rainfall data measures that from 8th august 2008, rainfall over study region increases beyond 150mm/day and peaks on 11th Aug. (387.7 mm/day). Therefore the event has been chosen as centred at 11th Aug. 2008. Fig 5.17 shows that the SST-rain correlation is low from 5 days prior of the event and WS-rain correlation improves from 2days prior of the event. All correlations are significant at 5% significance level. Correlation has been computed over all locations of AS for 5440 data points.

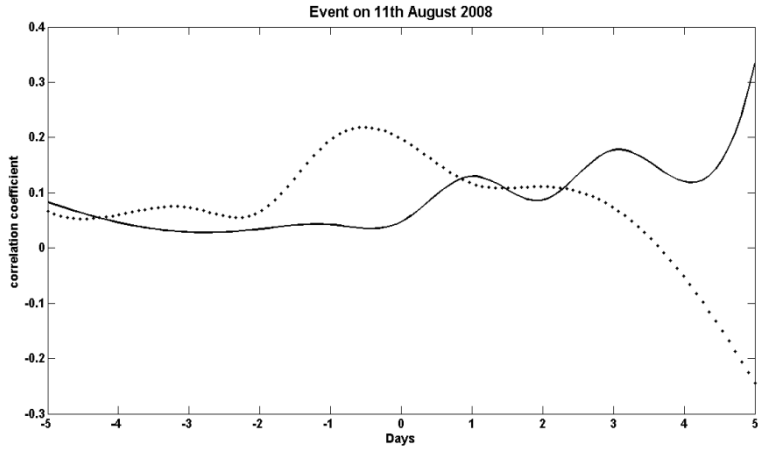

Figure 5.17 Extreme rain event on 11th August 2008, Y axis denotes correlation coefficient and X axis denotes number of days from the day of an event. Dotted line represents correlation between WS and rain while solid line is for SST and rain. 0th day is referred as the day of an event.

To investigate the spatial scale of propagation of high negative correlation between SST-rain and high positive correlation between WS-rain, the lagged correlation for prior and after 5 days

of extreme rainfall event has been estimated. For this cross-correlation calculations SST and WS have been kept as leading parameter and rainfall as lagging parameter. Fig. 5.17 displays correlation between WS-rain, SST-rain in time while fig. 5.18 & 5.19 shows the correlation between same parameters with respect to spatial locations. To study longitudinal (latitudinal) extend, all latitudes (longitudes) are averaged over some longitude [58°-75°E] (latitude [0°-20°N]). Y axis of fig. 5.18 & 5.19 indicates number of days by which one parameter is leading the other i.e. Y axis of fig. 5.18 indicates number of days by which WS is leading to rainfall. It has been observed that WS-rain correlation increases 2 days prior to 1 day after the event. The high positive correlation is confined to region between 8°-20°N in latitudinal direction i.e. whole WG region (fig 5.18a) and 70°-75°E in longitudinal extent i.e. west coast of India (fig 5.18b).

Similarly fig. 5.19 represents correlation between SST and rainfall for prior and after 5 days of the event. SST and rain correlation (fig. 5.19a) drops down to negative 3 days prior to the day of event (0 lag). The high negative correlation is from 14° to 20°N i.e. where extreme rain events have occurred from duration 1st to 20th August. SST-rain correlation in longitudinal direction (fig. 5.19b) shows from 3 days prior of the event SST-rain correlation decreases to low negative value and shifts from west to east AS i.e. near west coast of India. SST-rain correlation again increases to high positive value after a zero lag of the extreme rain event and it extents eastward direction.

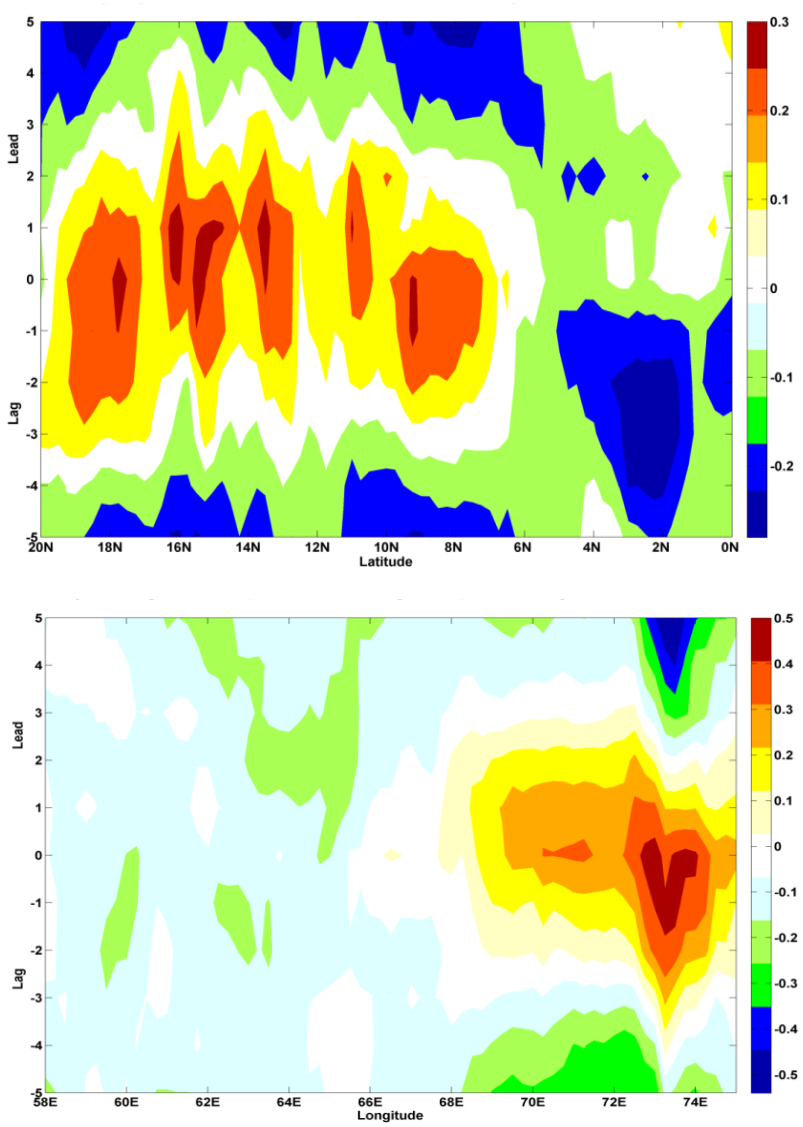

Figure 5.18 Cross correlation between WS and rainfall for 1st Aug to 20th Aug 2008. The extreme rain event is centered on 11th Aug. 2008 (0th day on Y axis). Here WS is leading rainfall. Colour bar indicates the correlation between WS and rainfall along a) Latitudinal direction b) Longitudinal direction. Red colour indicates high positive correlation while blue colour indicates high negative correlation.

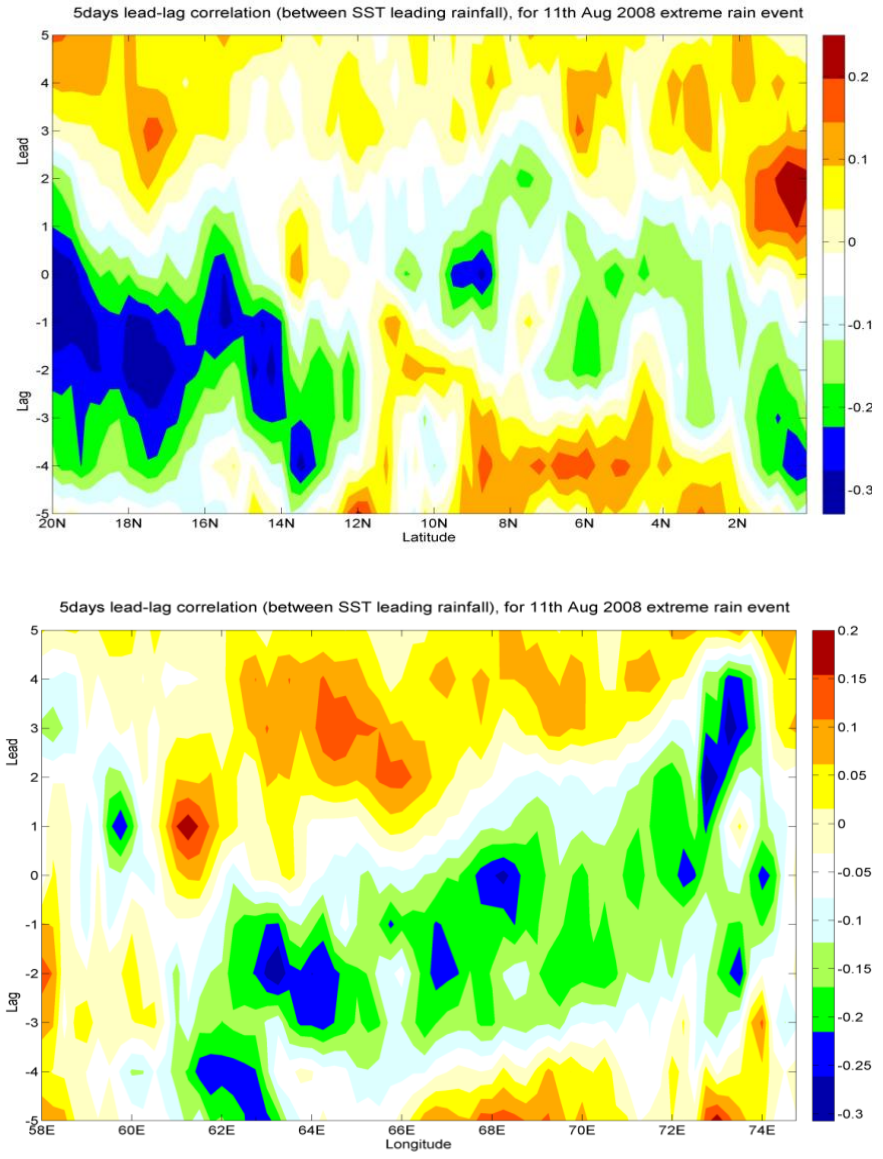

Figure 5.19 Cross correlation between SST and rainfall for 1st Aug to 20th Aug 2008. The extreme rain event is centered on 11th Aug. 2008 (0th day on Y axis). Here SST is leading rainfall. Colour bar indicates the correlation between SST and rainfall along a) Latitudinal direction b) Longitudinal direction. Red colour indicates high positive correlation while blue colour indicates high negative correlation.

Event 3: 10th July 2009

As per the IMD monsoon report (2009), an extreme rain event was recorded on 10th July 2009 near Maharashtra region with rainfall intensity 410 mm/day. TRMM 3B42 v7 satellite rainfall estimation gives 379mm/day rainfall on 9th July and 333.3 mm/day rainfall on 10th July 2009. Since the IMD rain gauge record is considered as the accurate measurement of rainfall, we have chosen 10th July as the day of extreme rainfall. Time series of correlation coefficients between SST-rain and WS-rain (fig 5.20) reveals that SST-rain correlation decreases from 3 days to 2 days prior the event, accompanied by increase in WS-rain correlation from negative to positive.

SST-rain correlation again decreases and WS-rain correlation increases from one day prior to one day after the event. All correlations are significant at 5% significance level. Correlation has been computed over all locations of AS for 5440 data points.

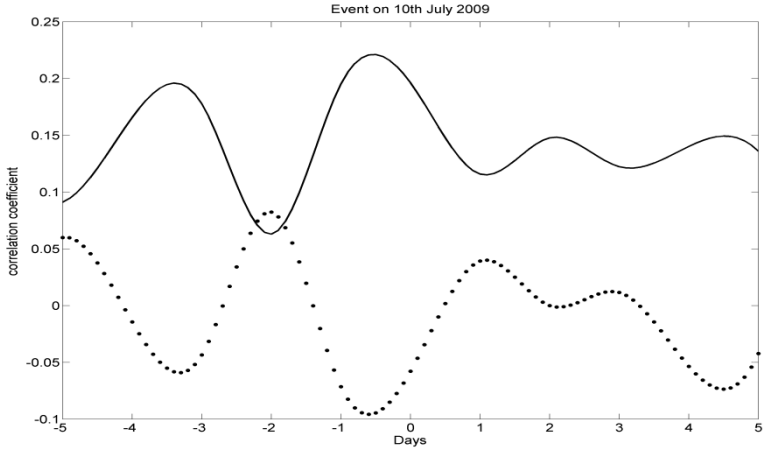

Figure 5.20 Extreme rain event on 10th July 2009, Y axis denotes correlation coefficient and X axis denotes number of days from the day of an event. Dotted line represents correlation between WS and rain while solid line is for SST and rain. 0th day is referred as the day of an event.

Event 4: 31st August 2010

According to IMD monsoon report (2010), there was an extreme downpour of the magnitude 480mm/day near coastal Maharashtra on 31st Aug 2010. TRMM 3B42 v7 satellite record shows 247.7mm/day rainfall on the same day and 279.76 mm/day on 30th Aug. As discussed in the analysis of earlier event that IMD rainfall measurements are presumed to be accurate as compared to satellite estimates, therefore 31th Aug. 2010 day is counted as the day of extreme rain event of year 2010. TRMM 3B42 v7 also informs the heavy downpour i.e. rainfall greater than 150mm/day, from 2 days prior to the event. Fig. 5.21 reveals that correlation between SST-rain decreases i.e. 0.3 on two days prior to the event and 0.03 on the day of an event. The correlation between WS-rain increases from 0.003 to 0.166 from two days prior an event to the day of an event. All correlations are significant at 5% significance level. Correlation has been computed over all locations of AS for 5440 data points.

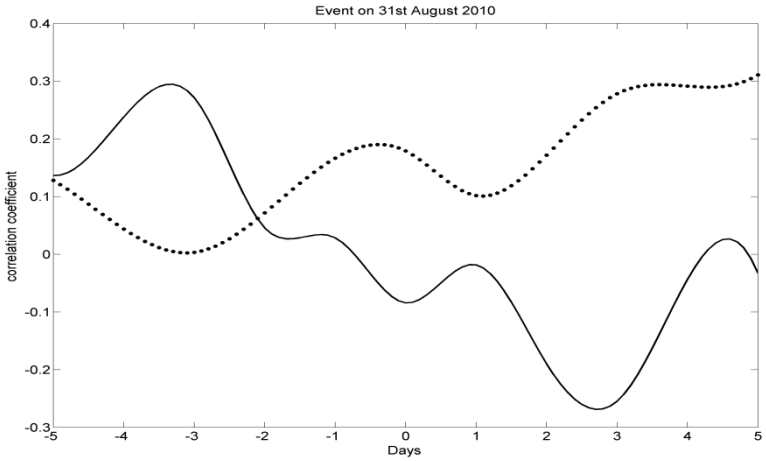

Figure 5.21 Extreme rain event on 31th August 2010, Y axis denotes correlation coefficient and X axis denotes number of days from the day of an event. Dotted line represents correlation between WS and rain while solid line is for SST and rain. 0th day is referred as the day of an event.

Event 5: 16th July 2011

IMD monsoon report (2011) has documented an intense rainfall event of 340 mm/day intensity near Maharashtra and Karnataka on date 16th July 2011. TRMM 3B42 v7 satellite also captures 361.4 mm/day rainfall on the same day. Temporal variation of correlation coefficient between WS-rain (fig.5.22), shows that correlation between WS-rain raises from 3 days prior the event and reaches maximum on one day before the event whereas correlation between SST-rain starts diminishing from 3 days prior to the event and reaches to minimum on one day before the event. Consequence of these variations in SST and WS leads to significantly increment in rainfall by an amount of 190mm on the day of the event. All correlations are significant at 5% significance level. Correlation has been computed over all locations of AS for 5440 data points.

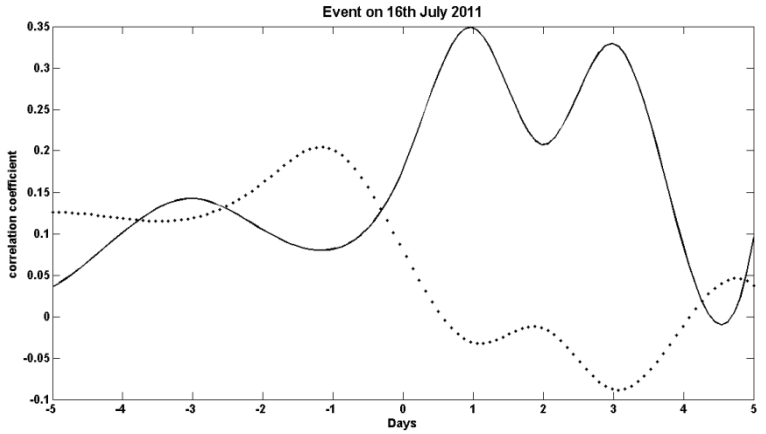

Figure 5.22 Extreme rain event on 16th July 2011, Y axis denotes correlation coefficient and X axis denotes number of days from the day of an event. Dotted line represents correlation between WS and rain while solid line is for SST and rain. 0th day is referred as the day of an event.

Event 6: 15th June 2012

TRMM 3B42 v7 rainfall measures an extreme rain event on 15th June 2012 with magnitude of 474.8mm/day (IMD report was not available at the time of analysis). This event is chosen for the analysis because rainfall greater than 150 mm/day is observed for all 11 days i.e. prior and after 5 days of an event with heaviest downpour on the day of that event. Fluctuations in correlation coefficient have been analysed for SST, WS and rain. Fig. 5.23 shows correlation between WS-rain increases from negative to positive from 3 days prior to one day after the event while correlation between SST-rain decreases from 3 days prior the event to the day of an event. It has been observed that after an event both WS-rain and SST-rain correlation increased i.e. in same phase and hence the rainfall of is found to be lesser after one day of an extreme rainfall event. All correlations are significant at 5% significance level. Correlation has been computed over all locations of AS for 5440 data points.

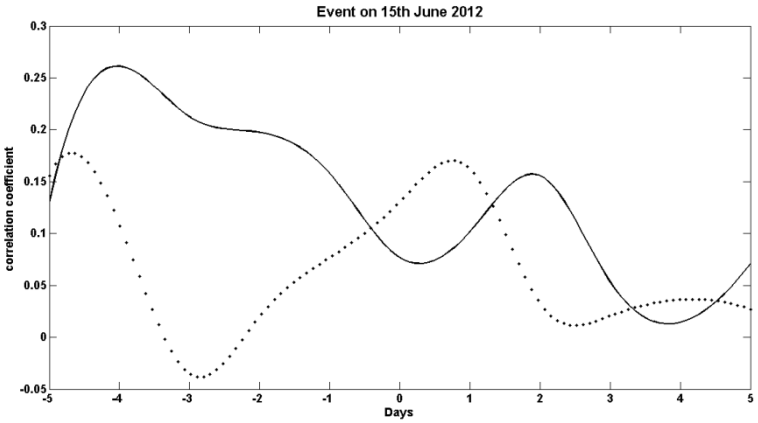

Figure 5.23 Extreme rain event on 15th June 2012, Y axis denotes correlation coefficient and X axis denotes number of days from the day of an event. Dotted line represents correlation between WS and rain while solid line is for SST and rain. 0th day is referred as the day of an event.

Results of all above figure suggests that before a very heavy downpour SST-rain correlation goes out of phase with that of WS-rain correlation i.e. SST-rain correlation decreases with increase in WS-rain over AS. The one possible mechanism behind this would be as follows, strong WS increases evaporation over AS and hence decreases AS SST. During this process the moisture availability in air parcels increases leading to a heavy precipitation over WG. Correlation between SST and rain steps down before 1 o 3 days of an extreme rain event. WS and rain correlation peaks before 1 to 3 days of an extreme rain event. Correlation has been computed over all locations of AS for 5440 data points (68 × 80 spatial locations).

Chapter 6. Conclusion and recommendation

Orographic aspects are key communicators to study enhanced precipitation and hence reason of unique biological richness of WG. For this purpose the remotely sensed rainfall data from TRMM 3B42 v7 has been utilized and validated with IMD rainfall gridded data sets. Spatial pattern of rainfall and rainfall variability considering annual and monthly scales captured by TRMM 3B42 v7 satellite estimates significantly matches with the IMD rainfall data over study region. The amplitude of rain intensity is underestimated by TRMM satellite data over WG barrier and slightly overestimated over rain shadow region. In future, to improve satellite data information of orographic rainfall over WG, it is recommended to utilize merge TRMM and rain gauge rainfall product introduced by Mitra et al. (2013).

The association of rainfall with orographic features over WG ratiocinate that the orographical rainfall is a coupled product of nature of topography, elevation of mountains and slope of barrier. The intensity of rainfall depends on the orographic parameters in the order shown by fig. 6.1, where most influencing orographic aspect placed at the bottom of triangle.

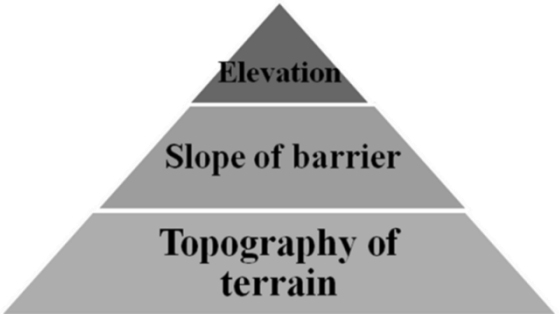

Figure 6.1 The interconnection between orographical aspects and intensity of orographic rain is shown in this triangle schematic. The most important component influencing the intensity of rainfall over WG is kept at the bottom of triangle.

Karnataka receives highest rainfall intensity compared to other states of WG. Also the leeward side of WG at Karnataka has strong rain shadow region compared to Maharashtra and Kerala. This is incorporated with terrain complexity of mountains in Karnataka. It satisfies all orographic aspects in adequate manner urging intense rainfall. Karnataka has broader and cascaded mountain barrier which impels effective spatial blocking of incoming flow and the apexes of sufficient elevation and gradually incrementing slopes which render intense rainfall. Orographic precipitation exacerbates before it reaches the peak and leeward side of the Mountain. In WG, intense orographic rainfall is confined up to 800 meter height. This suggests that there could be atmospheric blocking due to weak WS or temperature inversion layer. Validation of this boundary layer height over WG is suggested to carry out in future through radiosonde data. Though the rainfall in WG follows same spatial pattern in all the months of summer monsoon JJAS, frequency of heavy rainfall events is more in June, July as compared to August and September. Therefore it has been concluded that orography of WG doesn't

impact temporal variability in rainfall received over WG but it impacts on the spatial variability of rainfall over WG.

As per the validation results, TRMM 3B42 v7 rainfall estimates underestimate the heavy rainfall over WG of India. The new thresholds have been defined for TRMM 3B42 v7 rainfall data to classify heavy rainfall events over WG from PDF of 8 years (1998-2005) rainfall data. The two thresholds are as follows, 150>R>120 mm/day (99.5 percentile of the data) and R>150 mm/day (99.75 percentile of the data). Spatial distribution of rain events depicts that heavy rain events (150>R>120 mm/day) are likely to occur at Karnataka coastal region at frequency of approx. 2 events per year in south west monsoon. Unlikely, maximum number of extreme events with R>150 mm/day are prominently found at Maharashtra coast near Ratnagiri district (in a belt of 16° to 17° N). The lat-long of this spatial location at Maharashtra indicates vulnerable stations of Konkan railway in the vicinity which often faces landslide or derailment of boulders due to heavy downpour. Small dips in the elevation data in the vicinity of prone areas to extreme rain events have been observed. This observation further needs to be studied.

It has been observed that the trend in rainfall anomalies over WG varies in response to fluctuations in NINO 3.4 Index and DMI in south west monsoon season but the magnitude of rainfall over WG doesn't solely depends on ENSO and IOD events. Inteannual variation of seasonal mean monsoon rainfall over WG is primarily associated with of El Nino/La Nina and secondary with IOD events (large scale forcing) but daily variations in rainfall intensities i.e. extreme rain events are dependent on SST & WS over AS (regional scale effect). The trend analysis of ENSO cycle, IOD event with annual rainfall departure over WG suggests that El Nino with negative IOD suppresses the rainfall over WG while La Nina with positive IOD increases the rainfall over WG. There is connection between ENSO and rainfall over WG in summer monsoon season but ENSO events can't determine the strength of summer monsoon rainfall over WG. Monsoon over WG is not exclusively dependent on ENSO, IOD and AS SST. Though rainfall in JJAS over WG has some association with ENSO and IOD events but it has been observed that it doesn't ordain number of extreme rain events over WG. The AS state condition (SST, WS) has been analysed over oceanic region (58°-75°E, 0°-20°N) to study its association with local precipitation over WG. Correlation coefficients are calculated for 5440 (68 x 80 data points) spatial locations for SST & WS with rain. Variation of these three parameters for 5 days prior and after an extreme rain event has been observed for 6 events from year 2008 to 2012. It has been discovered that SST-rain correlation decreases while WS-rain correlation increases from 1 to 3 days prior to an extreme rain event. It may help to monitor the development of extreme rain event conditions by supervising SST, WS variations for consecutive 3 days. If both SST-rain and WS-rain correlation goes out of phase extreme rain event may be expected in 1 to 3 days of an observation. For concreteness of this relationship more number of extreme rainfall events should be observed in future. The present study will help to understand underlying mechanism that influences the orographic rainfall events over WG. It may help in preparedness for hazard management in future over WG. The results presented in this study are statistically significant nevertheless more studies coupled with general circulation models should be carried out to establish the robustness of the results.

References

Ajayamohan, R. S. & Rao, A. (2008). Indian Ocean dipole modulates the number of extreme rainfall events over India in a warming environment. Journal of the Meteorological society of Japan, vol. 86, No.1, pp. 245-252.

Basu, B. K. (2005). Some characteristics of model produced precipitation during summer monsoon over India. Journal of Applied Meteorology, vol.44, pp. 324-339.

Bhowmik, S. K. Roy & A. Das. (2007). Rainfall analysis for Indian Monsoon region using the merged rain gauge observations and satellite estimates: evaluation of monsoon rainfall features. Journal of Earth system sciences, 116, No.3, 187-198.

Bhowmik, S. K. R. & Durai, V. R. (2008). Multi-model ensemble forecasting of rainfall over Indian monsoon region. Atmosfera, vol.21, No.3, pp. 225-239.

Bookhagen, B. & D. Burbank. (2006). Topography, relief, and TRMM-derived rainfall variations along the Himalaya. Geophysical Research Letters, 33, L0840.

Clark, C. O., J. E. Cole, and P. J. Webster. (2000). Indian Ocean SST and Indian summer rainfall: Predictive relationships and their decadal variability. J. Climate, vol. 13, pp. 2503-2519.

Dash, S. K., M. Kulkarni, U. C. Mohanty, & K. Prasad. (2009). Changes in the characteristics of rain events in India. Journal of Geophysical Research, vol. 114.

De, U. S., and S. Dutta. (2005). West coast rainfall and convective instability. J. Ind. Geophys. Union, vol. 9, no.1, pp. 71-82.

Dept. of biotechnology Gov. of India & Dept. of Space Gov. of India. (2002). Biodiversity Characterisation at Landscape Level in Western Ghats India using satellite Remote Sensing and Geographic Information system.

Elliott, R. D., & Shaffer, R. W. (1962). The development of quantitative relationships between orographic and air-mass parameters for use in forecasting and cloud seeding evaluation. Journal of Applied Meteorology, vol.1, pp.218-228.

Elliott, R. D., & Hovind, E. L. (1964). The water balance of orographic clouds. Journal of Applied Meteorology, vol. 3, pp. 235–239.

Francis, P. A. & S. Gadgil. (2005). Intense Rainfall Events over the West coast of India. J. Meteorology and Atmospheric Physics.

Gadgil, S. (2003). The Indian monsoon and its variability. Annu. Rev. Earth Planet. Sci., vol. 31, pp. 429–67.

Goswami, B. B., P. Mukhopadhyay, R. Mahanta, and B.N. Goswami. (2010). Multiscale interaction with topography and extreme rainfall events in Northeast Indian region. Journal of Geophysical Research, vol. 115, D12114.

Goswami, B. N., V. Venugopal, D. Sengupta, M. S. Madhusoodanan and P. K. Xavier. (2006). Increasing trends of extreme rain events over India in a warming environment. Science, vol. 314, pp. 1442- 1445.

Grossman, R. L., and D. R. Durran. (1984). Interaction of low-level flow with the Western Ghats mountains and offshore convection in the summer monsoon. Mon. Weather Rev., vol. 112, pp. 652-672.

IMD monsoon report (2008), edited by Tyagi, A., Hatwar, H. R., & and Pai, D. S. National climate centre, Pune, IMD, Gov. of India.

IMD monsoon report (2009), edited by Tyagi, A., Hatwar, H. R., & and Pai, D. S. National climate centre, Pune, IMD, Gov. of India.

IMD monsoon report (2010), edited by Tyagi, A., Muzumdar, A. B., & and Pai, D. S. National climate centre, Pune, IMD, Gov. of India.

IMD monsoon report (2011), edited by Tyagi, A., & Pai, D. S. National climate centre, Pune, IMD, Gov. of India.

Izumo, T., Montegut, C. B., Luo, J. J., Behera, S. K., Masson, S., & Yamagata, T. (2008). The role of the Western AS Upwelling in Indian Monsoon Rainfall Variability. Americal Meteorological Society. Vol. 21, No.21, pp. 5603-5623.

Jaswal, A. K., Singh, V., & Bhambak, S. R. (2012). Relationship between sea surface temperature and surface air temperature over AS, Bay of Bengal and Indian Ocean. J. Ind. Geophys. Union , Vol.16, No.2, pp. 41-53.

Jiang, Q., & Smith, R.B. (2003). Cloud timescales and orographic precipitation. American Meteorological Society, vol. 60, pp. 1543-1559.

Kirshbaum, D. J., and R. B. Smith. (2008). Temperature and moist-stability effects on midlatitude orographic precipitation. Q.J.R. Meteorol. Soc., vol.134, pp.1183-1199.

Krishnakumar, K. N., P.G.S.L.H.V. Rao, and C. S. Gopakumar. (2009). Rainfall trends in twentieth century over Kerala, India. Atmospheric Environment, vol. 43, pp. 1940–1944.

Krishnamurthy, V., & Kinter, J. L.(2002). Global climate. Chapter: The Indian Monsoon and its Relation to Global Climate Variability, Springer-Verlag.

Konwar, M., A. Parekh, and B. N. Goswami. (2012). Dynamics of east-west asymmetry of ISMR trends in recent decades. Geophysical Research Letters, vol. 39, L10708.

Marwitz, J. D. (1980). Winter storms over the San Juan Mountains. Part I: Dynamical process. Journal of Applied Meteorology, vol. 19, No. 8, pp. 913–927.

Mitra, A. K., Bohra, A. K., Rajeevan, M. N., & Krishnamurti, T. N. (2009). Daily Indian precipitation analysis formed from a merge of rain-gauge data with the TRMM TMPA satellite derived rainfall estimates. Journal of the meteorological society of Japan, vol. 87A, pp. 265-279.

Mitra, A. K., Momin, I. M., Rajagopal, Basu, S., Rajeevan, M. N., & Krishnamurthi, T.N. (2013). Gridded Daily Indian monsoon rainfall for 14 seasons: Merged TRMM and IMD gauge analysed values. < http://www.ias.ac.in/jess/forthcoming/JESS-D-12-00332.pdf>

Moran, J. and Morgan. (1997). Meteorology-The Atmosphere & The Science of Weather, Prentice Hall publication London.

Mukherji, S., V. Srinivasan, and K. Ramamurthy. (1972). South west monsoon typical situations over Kerala and AS islands. IMD Forecasting manual, part II(3.8).

Nair, S., Shrinivasan, G., & Nemani, R. (2009). Evaluation of multi-satellite TRMM derived rainfall over a western state of India. Journal of the Meteorological society of Japan, vol. 87, no. 6, pp. 927-939.

Oruga, Y., and M. Yoshizaki. (1988). Numerical study of orographic-convective precipitation over eastern AS and the Ghat mountains during the summer monsoon. J. Atmos.Sci., vol. 45, pp. 2097-2121.

Patwardhan, S. K., and G. C. Asnani. (2000). Meso-scale distribution of summer monsoon rainfall near the Western Ghats (India). International Journal of Climatology, vol. 20, pp. 575-581.

Rahman, S. H., Sengupta, D., & Ravichandran, M. (2009). Variability of ISMR in daily data from gauge and satellite. Journal of geophysical research, vol. 114, pp. 1-14.

Raj, P. P. N., & P. A. Azeez. (2010). Changing rainfall in the Palakkad plains of South India. Atmósfera, vol. 23, no.1, pp. 75-82.

Rajeevan ,M., J. Bhate, and A. K. Jaswal. (2008). Analysis of variability and trends of extreme rainfall events over India using 104 years of gridded daily rainfall data. Geophysical Research Letters, vol. 35, L18707.

Rajeevan, M., & Bhate ,J. (2009). A high resolution daily gridded rainfall dataset (1971-2005) for mesoscale meteorological studies. Current Science, vol.91, No.4, pp.558-562.

Rajendran, K., A. Kitoh, J. Shrinivasan, R. Mizuta, and R. Krishnan. (2012). Monsoon circulation interaction with Western Ghats orography under climate change. Theor. Appl. Climatol., vol. 110, pp. 555–571.

Rao, K. J. and Goswami, B. N. (1988). Interannual variations of SST over the Arabian Sea and the Indian monsoon. A new perspective. Mon. Wea. Rev.,vol.116, pp.558-568.

Rao, S. A., Chaudhari, H. S., Pokhrel, S., & Goswami, B. N. (2010). Unusual central Indian drought of summer monsoon 2008: role of southern tropical Indian ocean warming. American meteorological society, vol. 23, pp. 5163- 5174.

Report of the Western Ghats Ecology Expert Panel, (31st August 2011), Submitted to the Ministry of Environment and Forests, Government of India.

Sabeerali, C. T., Rao, S. A., Ajayamohan, R. S., & Murtugudde, R. (2012). Climate dynamics, Vol. 39, pp. 841-859.

Saji, N. H., Goswami, B.N., Vinayachandran, P. N., & Yamagata,T. (1999). A dipole mode in tropical Indian Ocean. Nature, vol. 401, pp. 360-363.

Sarker, R. S. (1966). A Dynamical Model of Orographic Rainfall. Mon. Weather Rev., vol. 95, pp. 555-572.

Sengupta, D. B., Goswami, B. N., & Senan R. (2001). Coherent Intraseasonal Oscillations of Ocean and Atmosphere during the Asian Summer Monsoon. Geophysical research letter, vol. 28, no.21, pp. 4127-4130.

Shahi, N. R., Agarwal, N., Mathur, A. K., & Sarkar, A. (2011). Atmospheric correction for sea surface temperature retrieval from single thermal channel radiometer data onboard Kalpana satellite. J. Earth Syst. Sci., vol. 120, no. 3, pp. 337-345.

Shukla, J. (1975). Effect of Arabian sea-surface temperature anomaly on Indian summer monsoon: A numerical experiment with GFDL model.J. Atmos. Sci., vol. 32, pp. 503-511.

Shukla, J., & Mishra, B. M. (1977). Relationships between Sea Surface Temperature and Wind Speed over the Central AS, and Monsoon Rainfall over India. Monthly weather review. Vol. 105, pp.998-1002.

Simon, A. and Mohankumar, K. (2004). Spatial variability and rainfall characteristics of Kerala. Indian Acad. Sci. (Earth Planet. Sci.), vol. 113, no.2, pp. 211-221.

Smith, R. B., & Lin, Y. (1982). The addition of heat to a stratified airstream with application to the dynamics of orographic rain. Quart. J. R. Met. Soc., vol. 108, pp. 353-378.

Smith, R. B., & Evans J. P.(2007). Orographic precipitation and water vapour fraction over the Southern Andes. Journal of hydrometeorology, vol.8, pp. 3-19.

Smith, R. B., Schafer, P., Kirshbaum, D. J., & Regina, E. (2008). Orographic precipitation in the tropics: Experiments in Dominica. Journal of the atmospheric sciences, vol. 66, pp. 1698-1716.

Soman, M. K., K. Krishna Kumar, and N. Singh. (1988). Decreasing trend in the rainfall of Kerala. Current Science, vol. 57, pp.7-12.

Sumner, G. (1988). Precipitation: Processes and Analysis. (pp. 122-123). New York: John Wiley & Sons.

Suprit, K., and Shankar. (2008). Resolving Orographic Rainfall on Indian West Coast. International Journal of Climatology, vol. 28, no. 5, pp. 643-657.

Tewari, D. N. (1995). Western Ghats Ecosystem. (pp. 1-4). India, Dehradun: International Book Distributors.

Venkatesh, B., and Jose. (2007). Identification of homogeneous rainfall regimes in parts of Western Ghats region of Karnataka. Journal of Earth system science, vol. 116, issue 4, pp. 321-329.

Wallace, J. and P. Hobbs, 2006, Atmospheric science an introductory survey, *British Library Cataloguing-in-Publication Data*.

Yang, Y., & Chen, Y. L. (2008). Effects of terrain heights and sizes on island-scale circulations and rainfall for the island of Hawaii during HaRP. Mon.Wea. Rev., vol. 136, pp. 120-146.

<http://www.westernghatindia.org/>, accessed on 11th June 2012.

<http://www.meted.ucar.edu/>, sited on 16th October 2012.